Manuscript published in Archaeological Research in Asia 16: 148-165 (2018)

Bloomery iron smelting in the Daye County (Hubei): Technological traditions in Qing China

David Larreina-Garcia[a,*], Yanxiang Li[b], Yaxiong Liu[c], Marcos Martinón-Torres[d]

[a] Universidad del País Vasco (UPV-EHU), Miguel de Unamuno 3, 01006 Vitoria-Gasteiz, Spain

[b] Institute of Historical Metallurgy and Materials, University of Science and Technology Beijing, 30 Xueyuan Road, Haidian District, 100083 Beijing, China

[c] UCL Institute of Archaeology, London, UK, 31-34 Gordon Square, London WC1H0PY, UK

[d] Department of Archaeology, University of Cambridge, Downing Street, Cambridge CB23ER, UK

ABSTRACT

China is widely accepted as the birthplace and shrine of the blast furnace, with bloomery iron technology largely believed to be scant before the Han Dynasty, and virtually inexistent afterwards. Challenging this traditional picture, this paper presents the material characterisation and reverse engineering of the primary smelting of bloomery iron at five metal production sites, located in close proximity of each other in the Daye County in Hubei Province, China, and in operation during the middle Qing Dynasty.

A combination of materials science analyses–optical microscopy, SEM-EDS and WD-XRF–of surface collected technical material such as slags, furnace remains, and ores has demonstrated the established existence of bloomery iron at the core of the Chinese Empire. The five case studies present robust evidence of an overall broadly shared technical procedure based on the smelting of high grade ores in batteries of embanked furnaces, generating abundant slag but a limited metal output. The reconstruction of the various smelting processes in a relatively small region illustrates different technological adaptations to natural resources and socio-technological contexts, which are discussed using conceptual frameworks of rational economy and technological traditions.

1. Introduction

The temperature at which pure iron melts (*c.* 1550 °C) was out of reach for most ancient metallurgists; consequently, in most of the pre-modern world the extraction of metallic iron was typically achieved in the solid state at around 1200 °C, with the slag being the only liquid element. In simplified terms, this process involved reducing part of the iron oxides in the charge to form solid metallic particles that coalesced into a so-called bloom. The bloom, consisting of iron mixed with slag, required consolidation and refining through repeated hammering and annealing (smithing) to be workable. The iron produced by this method is called bloomery iron and the method itself is known as the direct method (Fig. 1). The other method used to smelt iron (known as the indirect process) involved the use of higher temperatures and more reducing conditions in a blast furnace; the product was a liquid state iron-carbon alloy which typically required a subsequent decarburisation treatment before it could be used (Rostoker and Bronson, 1990; Pleiner, 2000; Buchwald, 2005).

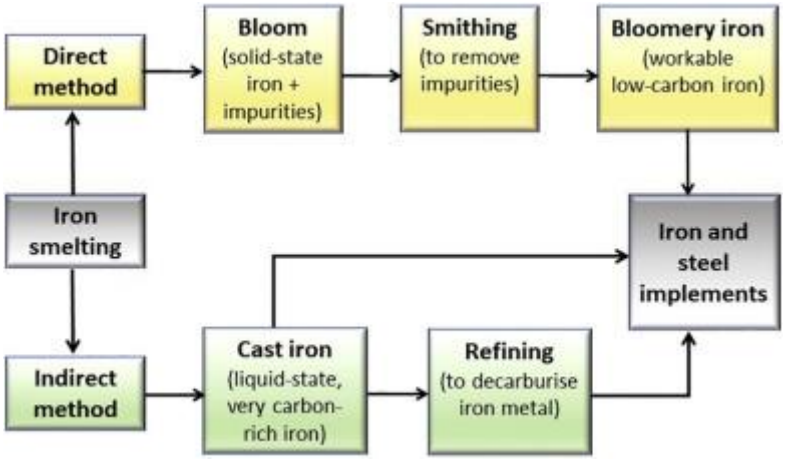

Fig. 1. Simplified flow chart showing the basic pathways of iron smelting by the direct and indirect methods.

As far as we know, China was the only world region that developed blast furnace technology before the 2nd millennium AD. The earliest cast iron fragment found so far in China is dated to the 8th century BC (Zou, 2000) whereas large quantities of excavated material show that cast iron production became the prevailing technique for iron metallurgy in the Central Plains of China no later than the 6th century BC (Han and Ko, 2007; Wagner, 2008; Chen, 2014; Liu et al., 2014). This is in stark contrast to the bloomery iron smelting tradition that predominated in most countries until relatively modern times.

Blast furnaces are more efficient than bloomery furnaces in terms of yield, since they can reduce most of the iron oxide in the charge and hence more metal is extracted per ore unit. Therefore, the indirect method is ideally suited for large-scale production. However, cast iron (typically containing *c.*3–4% C) is very brittle and hence only of limited application in its raw state. Thus, further techniques had to be developed by Chinese craftsmen to produce a malleable material, either by heat-treating and 'malleabilising´ the raw cast iron or, more frequently, by decarburising it and turning it into 'wrought iron' (≤1% C). This technology appears well established by the end of the Warring States period, around the 3rd century BC

(Wagner, 2008; Sun, 2009; Liu, 2016). Iron production was established at large-scale industrial complexes where the ore was reduced to metal, and foundries where objects such as horse fittings, woks, buckles, ploughs, etc. were mass-produced by stack-casting in moulds (Hua, 1983; Li, 1997).

This system was later inherited by the subsequent Han Dynasty and further improved, associated with a centralisation effort which ultimately derived into a monopoly policy that held the iron industry as a state-owned economy in the year 117 BCE. From that moment onwards, the production of iron outside imperial ironworks was forbidden and prosecuted (Sima, 1959; Wagner, 2001). Nonetheless, most imperial governments did not enforce the privilege over iron production. For example, during the Tang (618–906 CE), Song (960–1279 CE) and Ming (1368–1644 CE) dynasties, private production of iron was legitimised by paying tax to the government, and this system coexisted with the state-controlled production. During the Yuan dynasty (1279–1368 CE), even though private production of iron was formally banned, official production failed to meet the demand of the large domestic market, and the government tolerated the private production of iron (Yang, 1982, 182). New state ironworks were created at the beginning of the Ming period to better satisfy the increasing demand, but regulations were progressively introduced to encourage the participation of private smelters via licences and taxes (Li, 1982; Huang, 1989). At the end of the Ming period, most of the state ironworks were undermined by the great cost of production and complexity in the administration, and the demand of iron products was mostly met by private entrepreneurs (Wagner, 2008, 256). By 1743, the Qing emperor Qianlong opened completely the private mining of iron ores, which boosted the private mining and smelting of iron (Li, 2009). The Qing administration (1644–1912 CE), instead of monopolising production, issued a strict regulation over mining, smelting and trading of iron (Li, 2009). However, the production of iron declined during the last imperial dynasty, and by the end of the 19th century the competition with the foreign iron had ruined the iron industry of most regions within China (Wagner, 1997).

Regardless of the producer–state-owned or private sector–cast iron was the ‘workhorse’ material for most of China's history (Hua, 1983, 122). In spite of Wagner's (2008, 115ff) acknowledgement that both cast iron and bloomery iron smelting are believed to have co-existed under different circumstances for a long time, after the establishment of the Han monopoly over iron production, bloomery iron smelting is widely deemed to have become a rare, residual practice, while cast iron production in blast furnaces became the main smelting technique within China's cultural area (Huang and Li, 2013, 333).

The latter requires highly specialised craftsmanship and large amounts of labour force and infrastructure for mining, transportation, operation of the smelting, casting and finishing facilities. This large investment thus rendered cast iron production profitable only if there was relatively continuous, industrial-scale, regulated production. Conversely, bloomery iron smelting is a more adaptable technological procedure suitable for contexts where the above circumstances are not met. Overall, however, there is a scarcity of bloomery smelting evidence, artefacts made of bloomery iron are seldom recorded in central China, and most of the archaeological evidence of bloomery iron confirmed by scientific analyses is dated between 8th-3rd century BC, with the exception of an iron bar found in Gansu dated to the 14th century BC (Nanjing Museum, 1974; BUIST, 1975; Shandong Museum 1977; Changsha Railway Construction and Excavation Team, 1978; Liu and Zhu, 1981; Luo and Han, 1990; Xu et al., 1993; Bai, 1994; Han, 1998; Jiang, 1999; Zou, 2000; Chen et al., 2009, Chen et al., 2012; Liu et al., 2014).

The above picture is widely accepted, and it has been generally assumed that the direct method disappeared in favour of the indirect method, which offered an ideally suited model of production for the Chinese Empire: within a state that had mastered the necessary technological innovations, cast iron by blast furnaces ensured the supply of standardised products to large populations at competent prices, while a strong and stable administration controlled the production.

Adding complexity to this model, this paper demonstrates that bloomery iron smelting technologies run by independent producers did co-exist with the large state-owned ironworks and economies of scale in Imperial China. Specifically, we reveal a technological tradition of iron smelting by the direct method in the Daye County, Hubei Province, substantiated by the study of technical smelting remains from five ironmaking sites. We explain this tradition as a rational choice that was better suited for the socioeconomic and cultural context where it developed. Our study therefore challenges traditional generalisations whereby bloomery iron smelting is widely deemed to be a rarity in China due to the early development of the blast furnaces, and poses new directions and perspectives for future studies.

1.1 Archaeological background to the research area

Daye (大冶) is in the south-east of Hubei province, along the southwestern bank of one of the major bends in the Yangtze River (Fig. 2), an area very rich in both ferrous and non-ferrous minerals such as chrysocolla ($CuSiO_3.2H_2O$), malachite [$Cu_2CO_3(OH)_2$], azurite $Cu_3(CO_3)_2(OH)_2$, native copper (Cu), cuprite (Cu_2O), tenorite (CuO), haematite (Fe_2O_3), magnetite (Fe_3O_4) and andradite [$Ca_3Fe_2(SiO_4)_3$], as well as coal deposits, which were known from early times (Wagner, 1986, 3). Ruins of an ancient copper smelting and mining site were found at Tonglüshan and excavated between 1974 and 1985, indicating that there was continuous activity in the area during a 1000-year span throughout the entire 1st millennium BC (Huangshi Municipal Museum, 1999). Around 50 smelting sites have been documented near the main mining area, including some with tonnes of metallurgical residues and evidence of prolonged settlement (Hubei Provincial Bureau of Cultural Heritage, 2002, 42ff); these have generally been thought to be pre-imperial copper smelting sites. Before this study, no iron smelting activity had been documented archaeologically, although there are several written references related to iron mining in Daye in imperial documents of the Yuan, Ming, and Qing Dynasties, and the first modern Chinese ironworks–*Hanyeping Coal and Iron Company* (1889)–utilised ore from the Daye iron mines (Golas, 1999, 152ff; Wagner, 2008, 249ff; Wu, 2015, 106). As a matter of fact, the existence of a bloomery iron production tradition was a surprise discovery when analysing supposed copper slags for one of the case studies investigated here, but it was subsequently documented in four additional sites. Archaeometric analyses of material from eight sites documented two different metal productions in Daye, copper and bloomery iron, which coincide in space but are separated by a gap of about 2500 years (Larreina-Garcia, 2017). The present paper focuses solely on iron production.

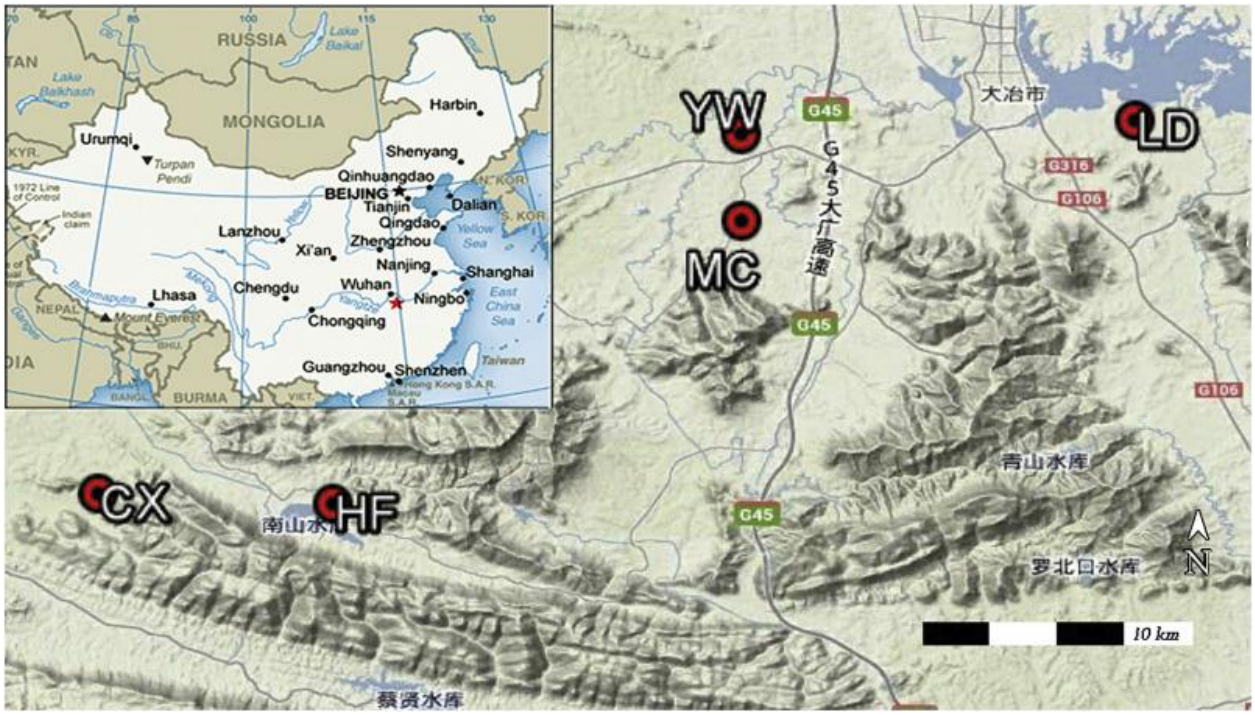

Fig. 2. Location of the case studies in Daye, the red star in the upper left corner map shows the location of the Daye County in Hubei province. China map courtesy of Perry-Castañeda library.

These iron smelting sites appear today covered by abundant vegetation, however an abundance of metallurgical residues can be recorded on the surface, including the predominant slag, and fragments of furnace wall and ore fragments. The five case studies are: Hongfengshuiku (HF) (洪枫水库), Maochengnao (MC) (茅城垴), Lidegui (LD) (李德贵), Yanwopu (YW) (燕窝铺) and Cangxiawu (CX) (仓下吴) (Fig. 2). The majority of the sites remain unexcavated, and the assemblages studied here were recovered from surface deposits during survey in May 2014, with the exception of few materials unearthed in the excavation of Lidegui and Hongfengshuiku in 2005 (Fig. 3).

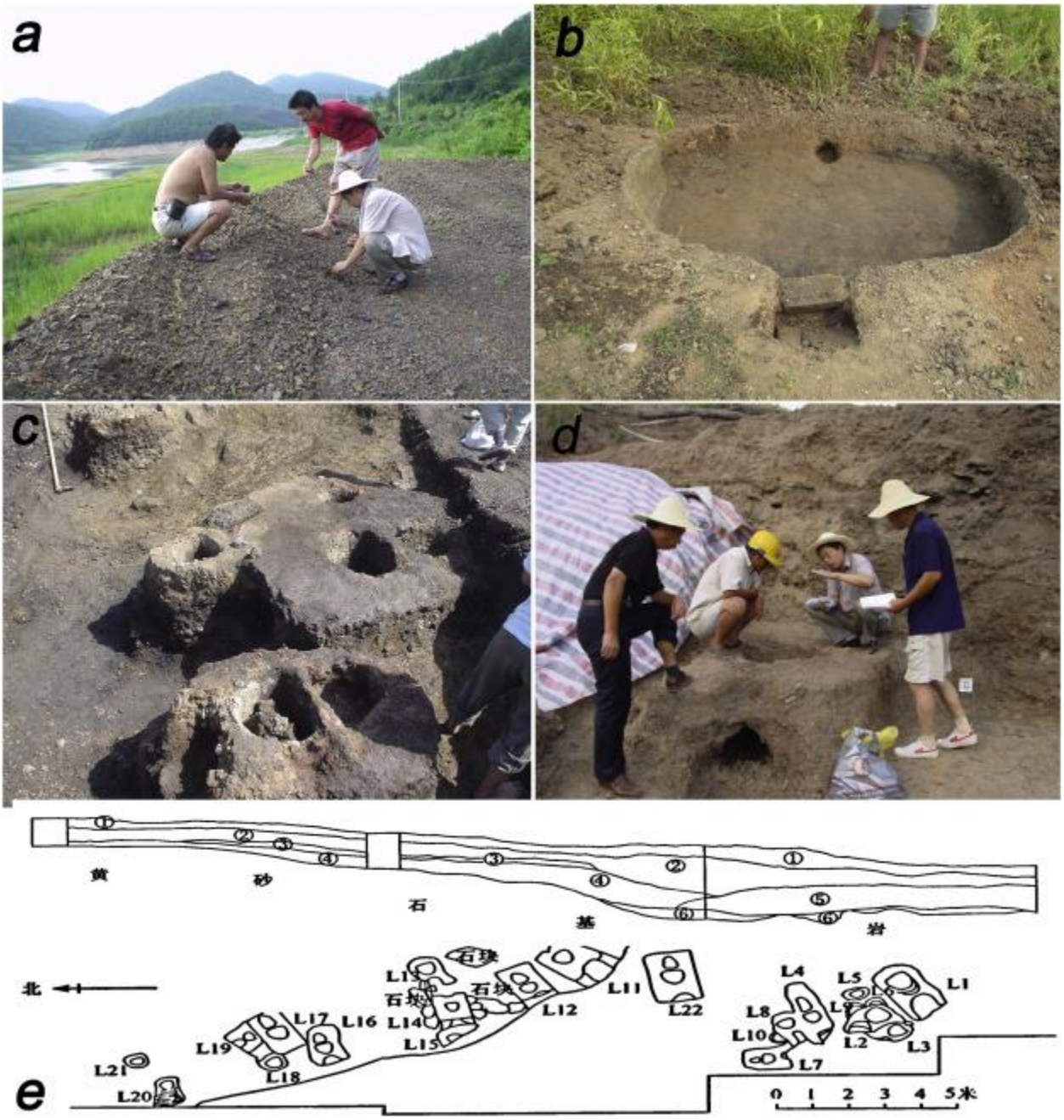

Fig. 3. Archaeological remains of HF and LD.

a) Large heap of slag found in 2005 and; b) porcelain kiln excavated in 2005 in HF, possibly active during the late Ming Dynasty; c) and d) excavation of furnaces in LD in progress; note the small size of the structures; e) Stratigraphic profile of LD, detailing the layers (up) and plan of the 22 furnaces (down), after Hu et al. (2013, Fig. 1, Fig. 2). Scale is in meters.

MC and YW appear catalogued in the Chinese Heritage Atlas of Hubei Province (Hubei Provincial Bureau of Cultural Heritage, 2002, 43, 48) as likely Zhou Period (1046–256 BCE) in date, and it is mentioned that the smelting installations span over large areas (*c.* 30,000 m^2), visible in large slag-heaps, areas of reddened soil and one furnace in MC; these structures were not visible in May 2014. CX does not appear in any archaeological register.

HF is not registered in the archaeologic 2002 Heritage Atlas either, since the site was discovered in 2005. The 2005 campaign identified one heap of slag of considerable dimensions, around 2 m high and over 5 m long (Fig. 3a). Close to the slag heaps were identified several larger rounded structures, one of which was excavated and identified as a porcelain kiln not associated to the metallurgical production (Fig. 3b). None of these structures were visible in 2014, however two metallurgical furnaces were visible in the natural section (Fig. 4), and a sequence of four samples of charcoal was extracted from one of them.

Fig. 4. Natural section showing the location of two furnaces in HF (pointed by arrows) and detail of the forehearths.

In May–July 2005, the Hubei Provincial Institute of Archaeology together with the Museum of Huangshi conducted a rescue excavation at LD in an area of 160 m^2 (Hu et al., 2013). Six stratigraphic layers were identified; levels 2–6 are dated to the Qing Dynasty while the top one corresponds to the current soil (Fig. 3e). Abundant slag–described in preliminary characterisation as a glassy matrix containing only fayalite crystals and wüstite (FeO)–was found in all layers. In addition, in the 3rd, 5th and 6th layers, were found 11, 10 and 1 furnaces respectively (Fig. 3c-e). Apart from the furnaces and the slag, charcoal, iron ore powder, fragments of furnace base lining, porcelain sherds were recovered; two iron bars were also found at this site.

1.2 Embanked furnaces

A total of 22 embanked furnaces arranged in battery were discovered at the site of LD (Fig. 3e): all of them showed a robust base with two clearly separated features: the furnace chamber

and forehearth on the one hand, and a working platform for the bellows at the rear on the other; the two features were connected by a tuyere hole of around 4 cm in diameter. Typically, the complete structure measures 80–90 cm in length (Fig. 5). The shaft is hopper-shaped and of small dimensions: the diameter at the top ranges 35–60 cm and 20–36 cm at the bottom, and the shaft is around 50 cm high. The largest dimensions are reached in furnace 22 with top and bottom diameters of 60 and 36 cm, respectively, and a shaft height of 54 cm. All the furnaces are entirely built up with clay; no other material, such as brick or stone was utilised (Hu et al., 2013, 294).

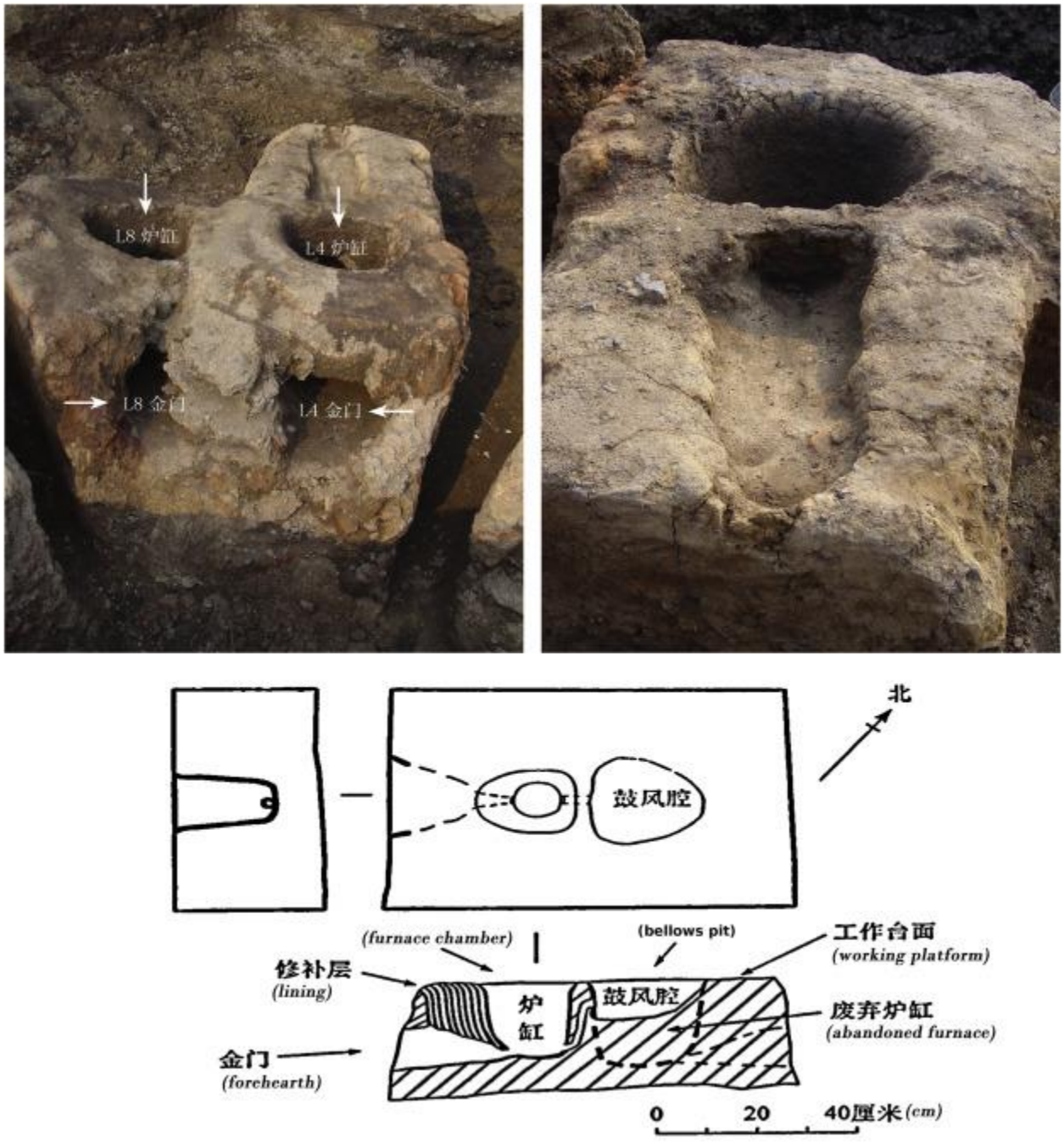

Fig. 5. LD furnaces during the excavation in 2005 and schematic plan of furnace 12. Forehearth (金门) and furnace hearth (炉缸) of furnaces 8 and 4, and working platform with the shallow

pit to accommodate the bellows in furnace number 4 seen from the back. Bottom: Plan and section of furnace 12 after Hu et al. (2013, Fig. 4).

The morphology of the LD structures is comparable to those found in 2014 in HF and visible in a natural section (Fig. 4). Even though these were largely obscured by vegetation and soil, the position of the shaft was evident since abundant charcoal demarcated an oblong shape perpendicular to the tapping holes, which were perfectly visible.

1.3 Radiocarbon dates

Seven charcoal samples of short-lived identifiable materials (plants and trees) were recovered in three of the sites–LD, HF and YW–from within smelting slag cakes and furnace base fills, and dated by radiocarbon (Supplementary Materials I). The results of all seven samples fall between the years 1643–1940 CE, although the samples concentrate in the period 1650–1800 with a probability of 75–90% (Table 1 and Fig. 6). The bulk of the results is internally consistent and in agreement with a further three radiocarbon dates obtained at the site of Lidegui: DLT1: 195 ± 40 BP (1643–1916); DLT2: 170 ± 40 BP (1644–1913); DLT3: 145 ± 40 BP (1667–1906) (Hu et al., 2013).

Lab. ID (sample)	Years BP	%	$\delta^{13}c$		Calibrated years AD		
OxA-31991 (HFC1)	199 ± 24	95.4	-23.73		1652–1684 (23.5%)	1735–1806 (51.4%)	1931… (20.5%)
OxA-31992 (HFC2)	213 ± 25	95.4	-26.88		1652–1684 (32.6%)	1735–1806 (47.2%)	1935… (15.6%)
OxA-31993 (HFC3)	212± 13	95.4	-23.78		1652–1684 (31.8%)	1735–1806 (47.6%)	1935… (16.0%)
OxA-31994 (HF2005)	190 ± 25	95.5	-26.10		1652–1684 (20.3%)	1735–1806 (53.7%)	1927… (21.5%)
OxA-31995 (LD001)	203 ± 25	95.4	-27.70		1652–1684 (25.8%)	1735–1806 (50.7%)	1934… (18.9%)
OxA-31996 (YW13)	239 ± 25	95.3	-25.30	1530–1539 (1%)	1652–1684 (58.5%)	1735–1806 (30.7%)	1940… (5.1%)
OxA-31997 (YW13b)	213 ± 24	95.4	-25.85	1643–1683 (33%)	1652–1684 (4.8%)	1735–1806 (41.9%)	1936… (15.7%)
OxA-31991 (HFC1)	199 ± 24	95.4	-23.73		1652–1684 (23.5%)	1735–1806 (51.4%)	1931… (20.5%)
OxA-31992 (HFC2)	213 ± 25	95.4	-26.88		1652–1684 (32.6%)	1735–1806 (47.2%)	1935… (15.6%)
OxA-31993 (HFC3)	212± 13	95.4	-23.78		1652–1684 (31.8%)	1735–1806 (47.6%)	1935… (16.0%)

OxA-31994 (HF2005)	190 ± 25	95.5	-26.10		1652–1684 (20.3%)	1735–1806 (53.7%)	1927… (21.5%)
OxA-31995 (LD001)	203 ± 25	95.4	-27.70		1652–1684 (25.8%)	1735–1806 (50.7%)	1934… (18.9%)
OxA-31996 (YW13)	239 ± 25	95.3	-25.30	1530–1539 (1%)	1652–1684 (58.5%)	1735–1806 (30.7%)	1940… (5.1%)
OxA-31997 (YW13b)	213 ± 24	95.4	-25.85	1643–1683 (33%)	1652–1684 (4.8%)	1735–1806 (41.9%)	1936… (15.7%)
OxA-31991 (HFC1)	199 ± 24	95.4	-23.73		1652–1684 (23.5%)	1735–1806 (51.4%)	1931… (20.5%)
OxA-31992 (HFC2)	213 ± 25	95.4	-26.88		1652–1684 (32.6%)	1735–1806 (47.2%)	1935… (15.6%)
OxA-31993 (HFC3)	212± 13	95.4	-23.78		1652–1684 (31.8%)	1735–1806 (47.6%)	1935… (16.0%)
OxA-31994 (HF2005)	190 ± 25	95.5	-26.10		1652–1684 (20.3%)	1735–1806 (53.7%)	1927… (21.5%)
OxA-31995 (LD001)	203 ± 25	95.4	-27.70		1652–1684 (25.8%)	1735–1806 (50.7%)	1934… (18.9%)
OxA-31996 (YW13)	239 ± 25	95.3	-25.30	1530–1539 (1%)	1652–1684 (58.5%)	1735–1806 (30.7%)	1940… (5.1%)
OxA-31997 (YW13b)	213 ± 24	95.4	-25.85	1643–1683 (33%)	1652–1684 (4.8%)	1735–1806 (41.9%)	1936… (15.7%)
OxA-31991 (HFC1)	199 ± 24	95.4	-23.73		1652–1684 (23.5%)	1735–1806 (51.4%)	1931… (20.5%)
OxA-31992 (HFC2)	213 ± 25	95.4	-26.88		1652–1684 (32.6%)	1735–1806 (47.2%)	1935… (15.6%)

https://c14.arch.ox.ac.uk/oxcal.html. OxCal v4.3.2 Bronk Ramsey (2017); r:5 INtCal13 atmospheric curve (Reimer et al. 2013). Check Supplementary Materials I for short-lived materials identification.

Table 1. ^{14}C results of the charcoal samples recovered from four sites in Daye.

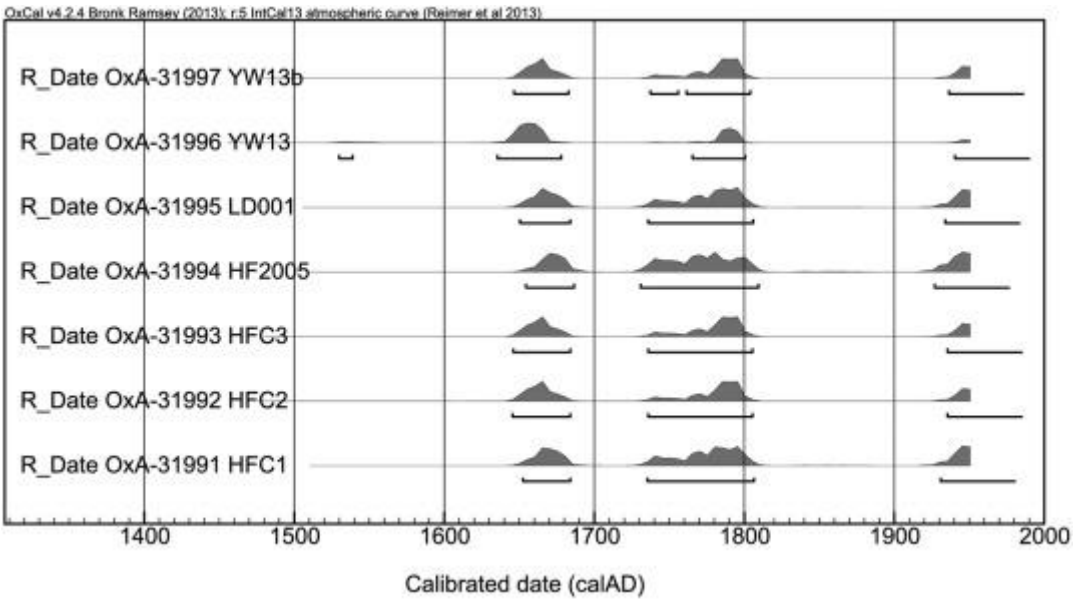

Fig. 6. Multiple plot showing the dates of the seven charcoal samples of Daye in calibrated years AD.

2. Analyses and results

Most of the material evidence analysed corresponds to tap smelting slag except for a few specimens (8 out of 47) which are bulky slag seemingly not tapped out of a furnace, and which are argued here to be smithing slag. The assemblage is completed by a few fragments of furnace wall and possible fragments of ore that were recovered in some of the sites (Table 2).

	HF	MC	LD	YW	CX	Total
Smelting slag	5	2	12	8	12	39
Smithing slag	5	2	1	–	–	8
Furnace wall	–	–	2	2	1	5
Ore	2	–	–	2	–	4

Table 2. Sampled materials per site associated to bloomery iron production.

2.1 Methodology

All the selected specimens from fieldwork were processed at the Institute of Historical Metallurgy and Materials (USTB) in Beijing whereas only sub-samples were exported to the UCL Wolfson Archaeological Science Laboratories in London for analyses. Prior to sampling, each specimen was recorded including dimensions, weight, macroscopic description, photographs and a magnetic test. The samples were mounted in epoxy resin and prepared by grinding on successively finer abrasive paper before being polished with diamond paste to a 1 µm finish, and the blocks were analysed by optical microscopy (OM) combining plane polarised light (PPL) and cross-polarised light (XPL) where appropriate. Unless otherwise

specified, all OM micrographs shown are PPL images. A JEOL 8600 Superprobe electron-probe microanalyser (EPMA) fitted with a back-scattered electron (BSE) and secondary electron (SE) detector for imaging, and energy-dispersive spectrometer (EDS) for compositional analysis was utilised for phase analysis to describe and analyse mineral phases and internal microstructures. A second piece of each sample of slag and ore, weighing 6 g–to ensure the necessary minimum of 4 g–was powdered in a planetary ball mill and pressed into a homogeneous pellet for bulk analyses by wavelength-dispersive X-ray fluorescence (WD-XRF) carried out at the University of Fribourg, using a Philips PW2400 sequential model. For the technical ceramics there was not enough material to perform the XRF analysis and instead the chemical composition was obtained by averaging chemical analyses of five areas (1 by 0.8 mm) per sample using SEM-EDS. Results of chemical analyses are presented as stoichiometric oxides, normalised to 100% by weight.

2.2 Technical ceramics

Furnace fragments were recovered at three sites: YW, CX and LD. In the former two sites, the fragments were recovered from different points scattered on surface without visible remains of the original foundations. In general, all samples are visually and compositionally quite similar (Fig. 7). They are bulky and amorphous, and typically display a gradient in section that is characteristic of furnace ceramics: from a grey-black reduced layer of frequently vitrified ceramic corresponding to the inner surface, to a layer of red-burnt clay with less severe signals of high temperatures (Martinón-Torres & Rehren 2014). Based on the chemical composition of the samples that appeared less altered by use, the preparation of technical ceramics seems to have followed a very similar recipe at all sites, based on the use of non-calcareous clays. The bulk chemical results of these ceramic fabrics reveal relatively low FeO (4–7%), moderate Al_2O_3 (9–10%) and high SiO_2 (77–84%). Other oxides range typically 1–2% although showing variation among samples (Table 3). The chemical composition of the more thermally altered ceramics shows higher FeO (8–10%), most likely from contamination from the charge.

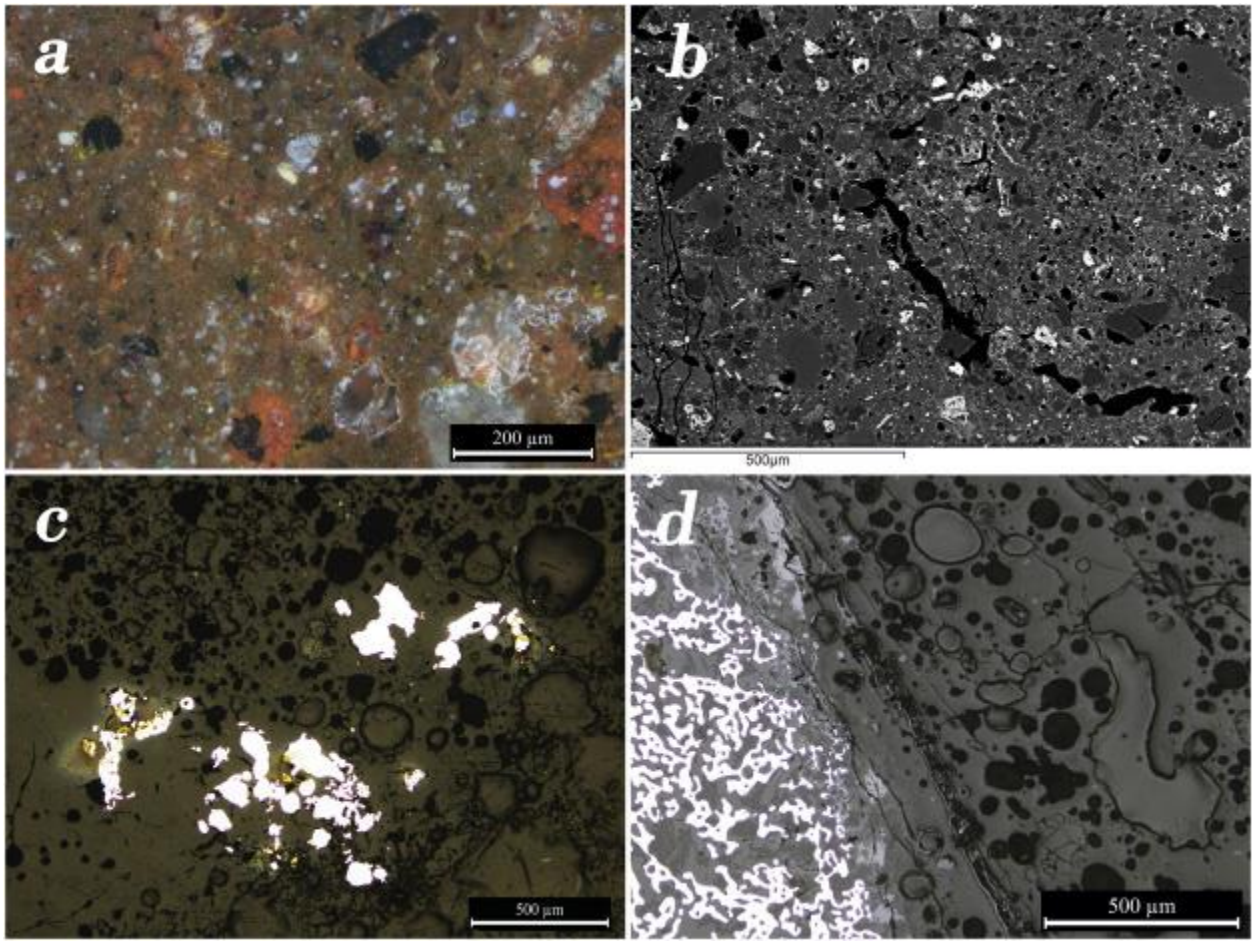

Fig. 7. OM and SEM micrographs showing the technical ceramics microstructure a) Detail (reflected XPL) of the red-burnt ceramic clay showing fine grains of quartz (white); b) SEM backscattered electron image showing larger grains of quartz and other minerals, some of them partially dissolved into the glassy matrix; c) Vitrified layer showing abundant porosity, slaggy areas and clusters of iron metal (white); d) Transition between the vitrified layer with iron corals and the strongly bloated ceramic fabric.

		Na_2O	MgO	Al_2O_3	SiO_2	K_2O	CaO	TiO_2	FeO
RED-BURNT FABRIC	YW9	bdl	0.9	9.0	77.0	3.4	2.2	0.8	6.8
	YW10	bdl	0.3	9.2	84.2	1.5	0.2	1.1	3.7
	LD10	0.4	0.4	9.8	81.1	2.0	0.2	0.8	5.1
	CX11	bdl	0.5	10.2	80.2	1.7	0.5	1.2	5.7
GREY-BLACK	YW9	0.2	0.9	9.4	74.8	2.1	2.1	1.1	10.1
	LD15	2.1	1.1	14.7	68.3	2.3	1.4	1.9	8.3
	CX11	bdl	0.5	9.8	76.6	1.7	0.5	1.0	10.0

Table 3. Bulk chemical composition of the bloomery iron furnace walls.

Fine rounded or semi-rounded quartz inclusions (100–300 µm) are frequent within the red-burnt clay (Fig. 7a), although towards the inner, more vitrified surface of the technical

ceramics quartz is more abundant and shows angular shapes (Fig. 7b), suggesting that the lining applied to the inner surface of the furnace was intentionally richer in crushed minerals. Here, not only quartz but also iron oxide minerals (possibly tailings from the ore) appear mixed with the clay, and these appear more cracked and shattered. Towards the inner surface, the latter minerals appear frequently partially reduced, with characteristic 'coral' bands of reduced metallic iron associated to iron oxides or silicates (Blomgren and Tholander, 1986) (Fig. 7d).

Due to the high melting temperature of silica (*c.* 1600 °C), the addition of this non-plastic temper increases the refractoriness of the clay (Freestone, 1986). Nonetheless, the ceramic seems have interacted chemically with the charge: frequently, these show glassy-slaggy areas where the quartz grains are mostly dissolved, occasionally recrystallising with iron-rich phases and, as mentioned, even reducing some iron from the silicates (Fig. 7c-d). This is likely due to the relatively low alumina and higher iron content of the clay, which would have rendered it less refractory.

2.3 Slag

Regardless of site, the bulk of the slag collection appears as relatively thin (20–40 mm) tablets; these show a homogenous, dense appearance in section which suggest that the slag was fully molten (Fig. 8a-c). Their flat shape, distinct smooth upper face with evidence of flowing and rough bottom face with occasional soil or imprints of soil particles, are diagnostic of slag that was tapped out of the furnace (e.g. Maldonado and Rehren, 2009).

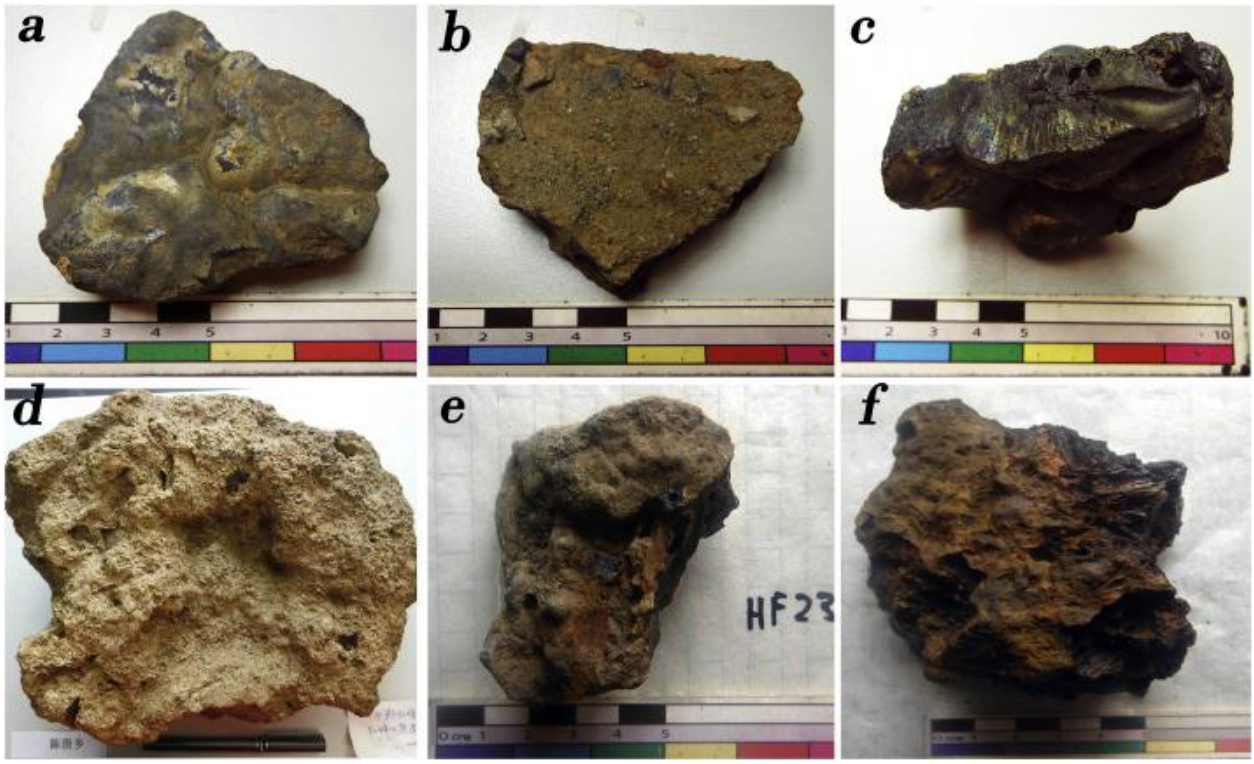

Fig. 8. Typical appearance of the Daye bloomery iron slag.

a-c) Top, bottom and section of the typical iron tap smelting slag; d) Complete specimen displaying charcoal and imprints of charcoal (not sampled); e) Plano-convex cake showing smooth surfaces; f) Bulky cake showing heavy rusty tarnish and abundant imprints of charcoal.

The bulk chemical composition of the Daye iron slag is fayalitic, ranging 62–71% FeO and 20–25% SiO_2. Al_2O_3 is the third major oxide (4–6%) in all cases. When SiO_2, FeO and Al_2O_3 are added up, they make up over the 95% of the bulk (Table 4). All other compounds are present in minor amounts with the exception of CaO, which can reach up to 3–4% in some specimens, Cu typically appears at trace levels and only rarely reaches >100 ppm. The notable exception is sample YW4, with a Cu content of >5000 ppm. This sample presents identical bloomery iron microstructure to the other specimens in Daye, and the most likely explanation is that the high levels of Cu are due to ore contamination, given the abundance of copper-bearing minerals in the region reported above (Table 4).

	MgO	Al_2O_3	SiO_2	P_2O_5	SO_3	K_2O	CaO	TiO_2	MnO	FeO	Cu*
HF MEAN (5)	0.5	5.2	21.4	0.2	0.1	0.9	1.0	0.2	0.2	70.3	53
MEDIAN	0.6	5.2	21.1	0.2	0.1	0.8	0.9	0.2	0.1	70.0	68
STD DEV	0.1	0.4	3.0	0.1	0.01	0.2	0.3	0.02	0.03	3.4	37
MAX	0.6	6.0	26.6	0.3	0.1	1.1	1.5	0.2	0.2	75.5	91
MIN	0.4	4.6	17.5	0.1	0.1	0.7	0.7	0.1	0.1	65.1	bdl
MC6**	0.9	6.7	19.3	0.4	0.1	1.1	3.1	0.2	0.3	68.1	536
MC1**	0.3	4.5	19.9	0.1	0.1	0.8	0.8	0.2	0.1	73.2	bdl
LD MEAN (12)	0.4	4.1	20.5	0.3	0.1	1.0	1.6	0.2	0.2	71.6	52
MEDIAN	0.5	3.9	20.3	0.3	0.1	1.1	1.4	0.2	0.1	72.5	8
STD DEV	0.1	0.7	2.8	0.1	0.03	0.3	0.8	0.1	0.1	4.4	88
MAX	0.6	5.7	25.2	0.4	0.13	1.4	2.8	0.3	0.3	78.2	318
MIN	0.2	3.4	16.0	0.2	0.04	0.3	0.4	0.1	0.1	64.8	bdl
YW MEAN (8)	0.5	4.5	20.0	0.2	0.1	0.7	1.0	0.2	0.1	72.5	81
MEDIAN	0.7	4.6	20.4	0.5	0.1	0.7	1.6	0.2	0.2	71.0	806
STD DEV	0.4	0.5	2.8	0.7	0.1	0.1	1.4	0.03	0.3	5.4	1819
MAX	1.7	5.7	24.9	2.1	0.2	0.9	4.9	0.2	0.9	77.3	5260
MIN	0.5	4.1	15.5	0.1	0.1	0.5	0.6	0.2	0.1	59.4	bdl
CX MEAN (12)	0.5	4.4	21.3	0.2	0.1	0.6	0.7	0.2	0.1	71.8	20.0
MEDIAN	0.5	4.3	20.8	0.2	0.1	0.6	0.7	0.2	0.1	72.4	5.0
STD DEV	0.1	0.5	2.3	0.03	0.01	0.1	0.2	0.03	0.03	3.0	28.8
MAX	0.6	5.3	25.7	0.2	0.1	0.7	1.1	0.2	0.2	77.1	81
MIN	0.4	3.5	17.7	0.1	0.03	0.4	0.5	0.2	0.1	67.0	bdl

*All values in % except Cu (ppm). **Median and standard deviation not calculated since the sample consisted of two specimens only. Check Supplementary materials II for full results and CRMs.

Table 4. WD-XRF chemical composition of Daye bloomery iron tap slag.

Fayalite is the only silicate that crystallised out of the glassy matrix, and it regularly contains some MgO (1–2%). It typically occurs as closely-spaced laths, which are occasionally interrupted by scant areas of glassy matrix (Fig. 9a-b).

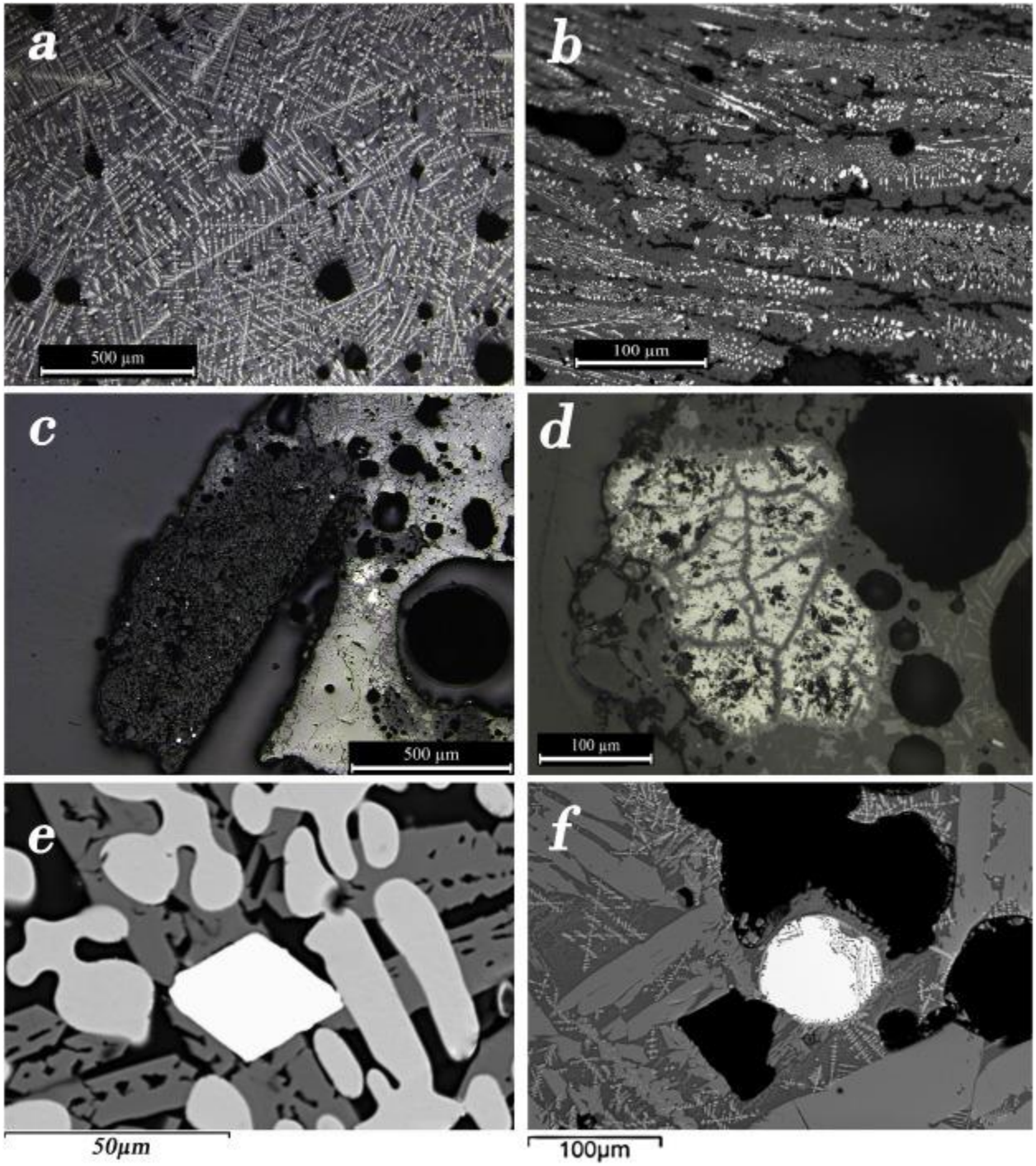

Fig. 9. OM and SEM micrographs showing the typical microstructure of the Daye bloomery tap slag.

a, b) Typical microstructure showing fayalite-wüstite eutectic with predominant elongated olivines (medium grey) crossed by dendritic wüstite (light grey or white), and occasional tiny iron metal particles (bright white); c) Argillaceous material (dark grey) attached to the outer

surface of the specimen showing limited interaction with the slag; d) Detail of residual magnetite (bright grey); e) BSE micrograph showing detail of dendritic wüstite (bright grey) and an iron particle (white) over fayalite laths (dark grey); f) BSE micrograph showing a larger rounded metal particle.

The most abundant iron oxide is wüstite, which is by far the dominant iron oxide within the microstructure of the tap slag, crystallising as dendrites (Fig. 9). Other iron oxides are scarce in comparison: cubic shapes or pseudomorphs of magnetite are rare and usually constrained to the oxidised boundary that separates consecutive runs of slag, and hence denote locally oxidising conditions during cooling, after the slag was tapped.

In general, metallic iron particles are not very abundant in the Daye slag; as a matter of fact these are absent in 18 out of 39 specimens, representing 46% of the tap slag sample. When present, they are sub-angular or sub-rounded small particles (≤30 μm) albeit with larger exceptions (Fig. 9e), and occasionally they are shaped as rounded and larger globules (Fig. 9f). Selected samples were etched in order to reveal grain textures and determine the type of iron alloy. None of the iron particles revealed any crystal, or they showed light grain boundaries corresponding to low carbon steel reduced in the solid state.

Residual quartz and argillaceous materials are very rare within the slag, and they correspond to patches of clay likely absorbed from the furnace walls; these are typically attached to the slag surface, presenting sharp interfaces and little interaction with the slag (Fig. 9c). Other residual materials, also exceptional, are chunks of haematite normally showing signals of advanced reactions: i.e. embedded in the matrix, with cracks filled by slag, or as agglomerations of re-crystallised iron oxide pseudomorphs of the parent mineral (Fig. 9d).

2.3.1 Smithing slag

In general, these appear in the form of amorphous bulky cakes uniformly covered by an orange-brown rusty tarnish, showing occasional vitrified patches and charcoal inclusions or impressions, which are totally absent in the tap slag (Fig. 8e-f). All these slag specimens show abundant gas cavities (1–3 cm) in section, orange-reddish stains, and brittle consistency. One specimen recovered during the archaeological excavation in LD fits easily into the defining characteristics of a ‘calotte’ or ‘smithing hearth bottom’, shaped as an elliptic plano-convex cake of around 16 cm in diameter and 2 kg in weight; the top side displays glazed parts, ridges and a characteristic depression caused by the blast of air (Serneels and Perret, 2003; Buchwald, 2005) (Fig. 10). In general, the smithing slag samples show a bulk composition comparable to the tap slag, although typically richer in FeO (3–5% more) with a corresponding decrease in SiO_2. The composition of the smithing slags shows higher inter-site variability than smelting slags (Fig. 11).

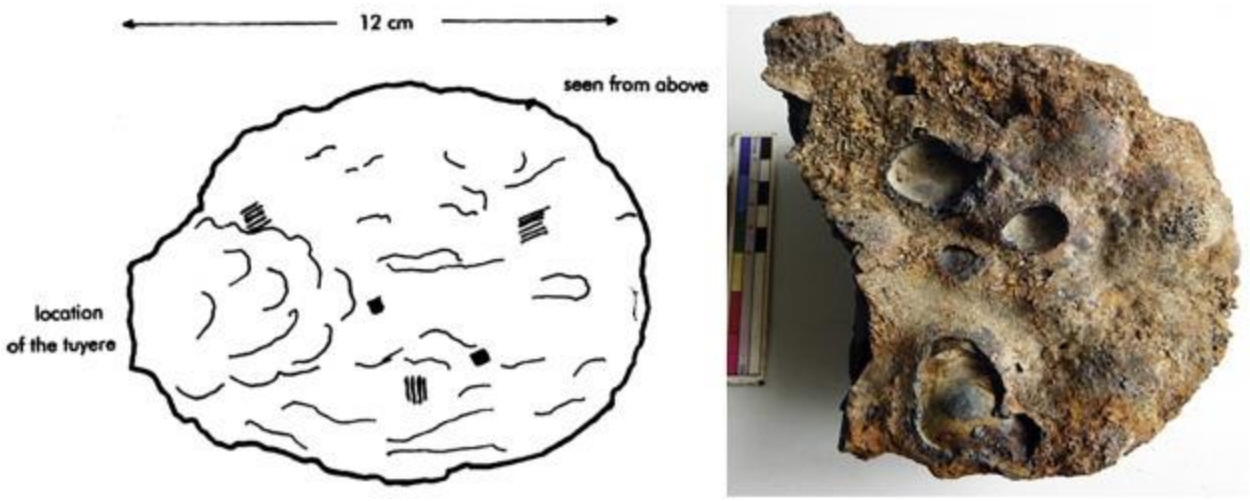

Fig. 10. Top view of a calotte slag type and top view of specimen LD11.

After Buchwald (2005, Fig. 91). Scale is 10 cm in LD photograph.

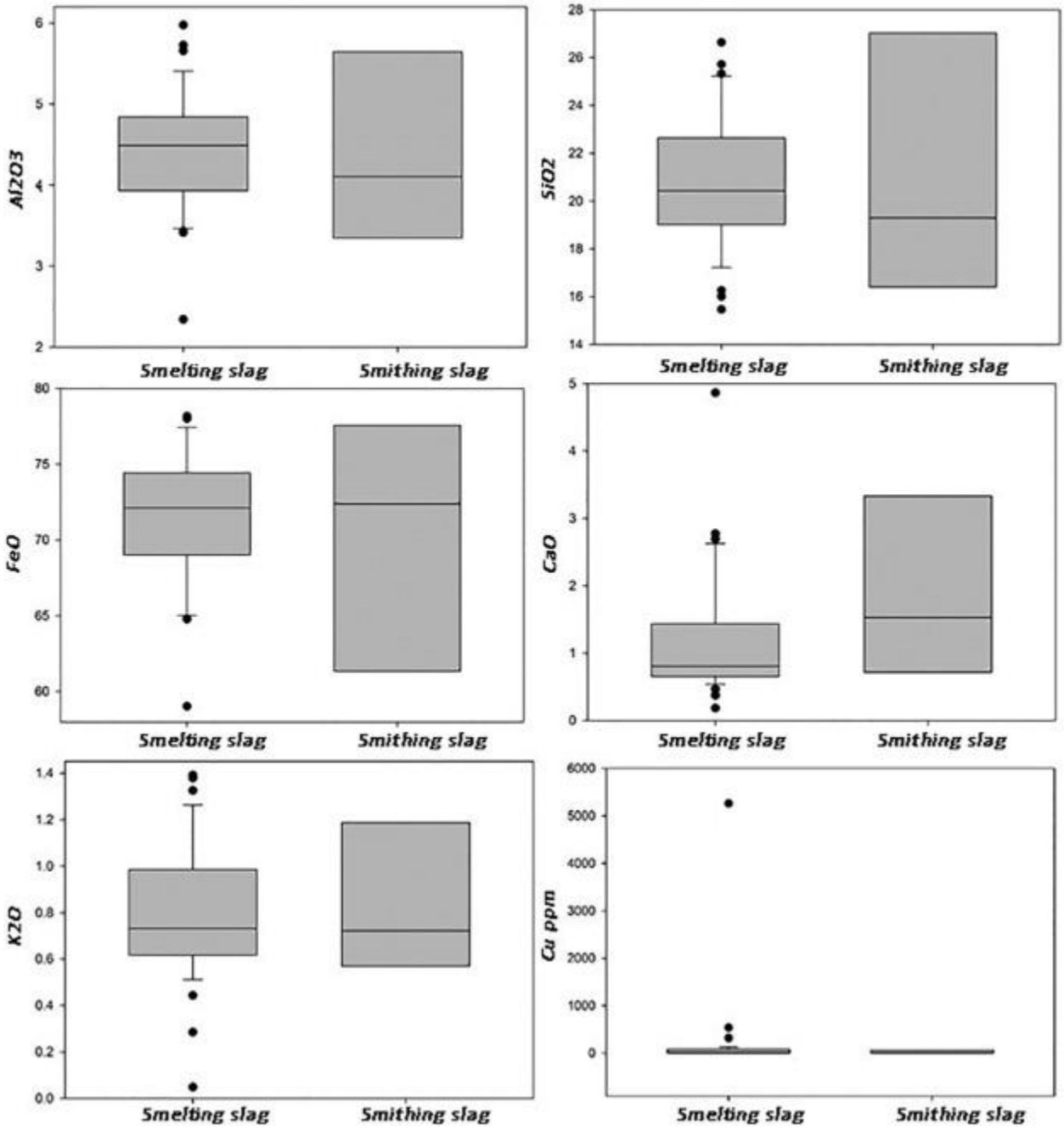

Fig. 11. Box, median and whiskers comparing relevant oxides in bulk composition (WD-XRF) of smelting and smithing slag.

The typical texture of this slag is heterogeneous, showing intergrowths of predominant dendritic wüstite and scant areas of olivines (fayalite) spotted by abundant porosity and corrosion products, with occasional areas fully covered by thick globules of wüstite, massive silicates, remnants of charcoal; metallic iron is very rare but where present it occurs as larger particles and, occasionally, as clusters (Fig. 12).

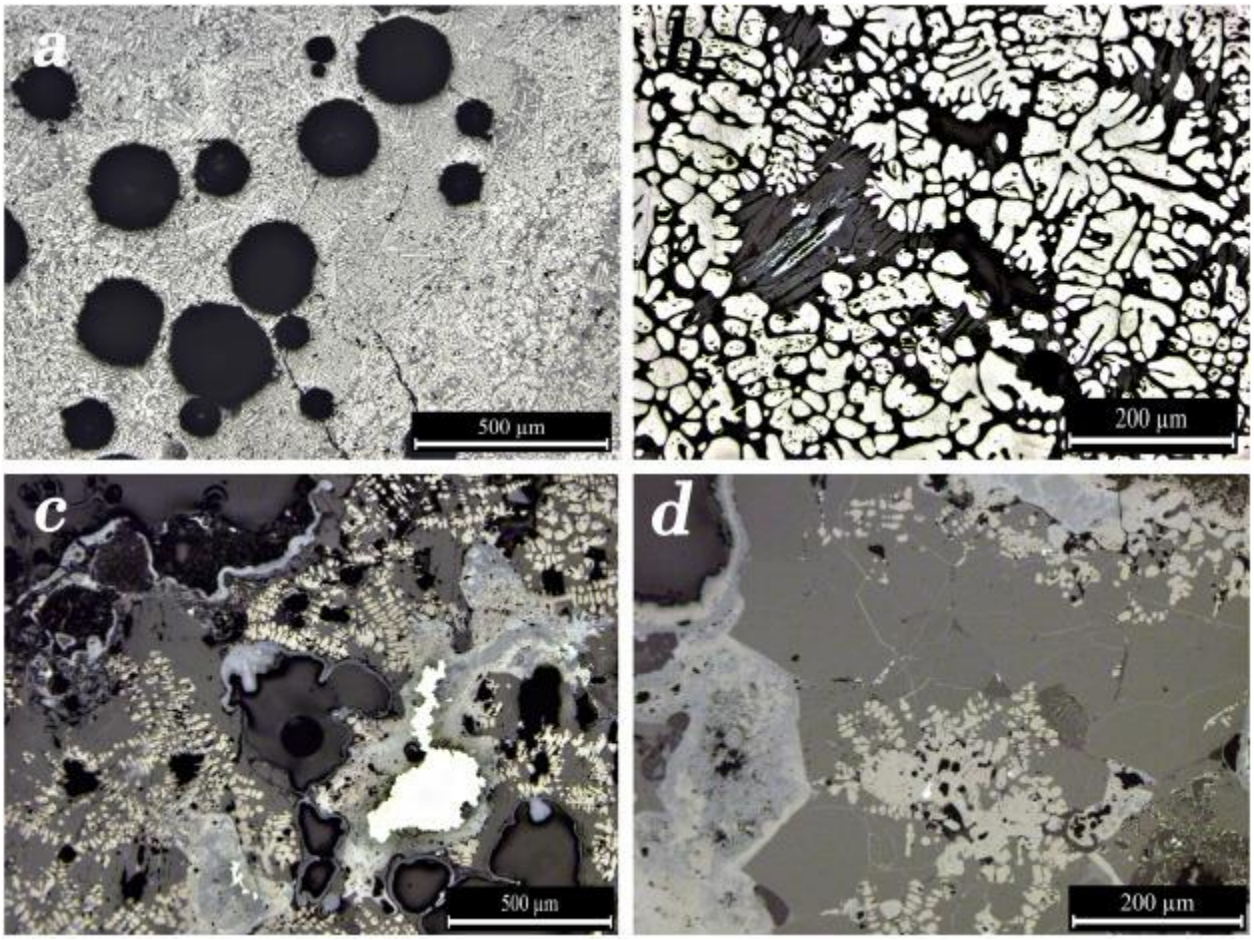

Fig. 12. OM micrographs showing the typical microstructure and olivines appearance in the Daye bloomery smithing slag.

a) Typical texture of the lumpy slag showing intergrowths of predominant dendritic wüstite and scant visible areas of olivines, and abundant porosity; b) Detail of olivine laths (dark grey) and thick globules of wüstite (white); c) Very large agglomeration of iron metal (bright white) surrounded by abundant corrosion products (light grey-bluish), wüstite (white grey) and iron silicates (dark grey); d) Detail of massive olivines (dark grey) between corrosion products (light grey, bluish), and agglomerations of wüstite (light grey) with few iron metal particles (white).

Even though discerning smelting from smithing slag can be challenging, morphological, compositional and mineralogical criteria allow for a distinction between both slag types when the whole assemblage is considered (Serneels and Perret, 2003; Buchwald, 2005; Erb-Satullo and Walton, 2017): 1) the smelting slag appears as relatively thin cakes with evidence of flow, whereas the smithing slag mostly corresponds to irregular chunks of undiagnostic shapes and brittle appearance, with imprints of charcoal and an oxidation crust; 2) the smithing slag shows an heterogeneous and highly vesicular cross-section, compared to the denser and homogeneous smelting slag; 3) the smithing slag tends to be slightly richer in FeO and shows more inter-site variability in chemical composition; 4) the smelting slag invariably exhibits a characteristic microstructure of fayalite laths, dendritic wüstite and scant iron particles, whereas the smithing slag shows a more heterogeneous crystal structure, very rich in iron oxides similar to hammerscale combined with crystalline areas free of those, partially reacted

materials, abundant corrosion and oxidation products, and scant clusters of metallic iron that could correspond to small pieces of iron breaking off during smithing. Finally, the two bars of iron recovered in LD (Hu et al., 2013) are supportive of our interpretation, as an iron billet or bar is a common kind of product obtained by primary smithing.

2.4 Ore

Possible fragments of ore, found associated to slag heaps, were sampled only at two sites: HF and YW. Most of them show a variety of dull to bright red colours, frequently with reddish-brown or blood red reflections. These colours and the friable consistency can sometimes be taken as indicative of roasting (Fillery-Travis, 2015, 268). Iron ore powder was found in abundance during the excavation of Lidegui (Hu et al., 2013), and thus it is conceivable that the ore was roasted prior to crushing. The ore samples analysed are quite rich in iron oxide (78–95% as FeO) (Table 5). Three of the fragments were characterised by X-ray diffraction and found to be dominated by haematite and magnetite, respectively.

	MgO	Al_2O_3	SiO_2	SO_3	K_2O	CaO	TiO_2	FeO	Cu*	XRD analysis
HF27	bdl	1.0	3.7	bdl	bdl	bdl	bdl	95.0	647	Haematite
HF29	2.4	2.1	5.9	7.0	0.1	1.1	0.1	81.1	832	Magnetite
YW11	0.2	2.3	18.9	bdl	bdl	0.2	bdl	78.1	bdl	Haematite
YW12	0.1	1.8	7.5	0.1	bdl	0.1	0.1	90.2	598	–

*Cu in ppm. Difractograms are available in Supplementary materials III.

Table 5. WD-XRF results of mineral samples (relevant oxides only).

3. Discussion

3.1 Technical interpretation

The interpretation of the tap slag from Daye as deriving from bloomery iron smelting is straightforward and unequivocal: the crystalline matrix with olivines; the fayalitic bulk chemical composition of 57–78% FeO and 15–31% SiO_2; dominant dendritic wüstite indicative of highly reducing environment (more reducing than required to smelt copper); the fact that the only metallic particles are very low carbon iron; and very low levels of any non-ferrous heavy metal; altogether clearly indicate that this is a waste product of bloomery iron smelting activities comparable in morphology, microstructure and composition to bloomery iron slag from Africa (e.g. Miller and Killick, 2004), Northern Europe, (e.g. Espelund, 2015) or Southeast Asia (e.g. Chuenpee et al., 2014). The few production remains with diagnostic characteristics of smithing slag also support the interpretation of the assemblage as debris of iron reduced by the direct method.

The shape of metallic iron micrograins is a reliable indicator of the furnace reduction conditions. In particular, the angular grains predominant within the Daye slag are indicative of reduction in the solid state in a low bloomery furnace (Blomgren and Tholander, 1986), which agrees with the furnace types found at some of the sites (Fig. 4 and Fig. 5). As mentioned, in addition to the irregular grains some specimens also present globular droplets. These are less commonly produced in a low bloomery furnace, yet it is perfectly possible to generate liquid

iron occasionally using this furnace type (Crew et al., 2011 and literature therein) (Fig. 9e-f). Importantly, the Daye slag does not show any of the diagnostic features of blast furnace debris, which is described as viscous slag showing bright rather than matte colours, and presenting a cryptocrystalline microstructure consisting only of few perfectly rounded C-rich iron prills suspended in the glassy matrix; furthermore, the chemical composition of cast iron slag is notably poorer in FeO, and typically richer in CaO (White, 1980; Rehren and Ganzelewski, 1995; Buchwald, 2005, 158–159).

Lastly, cast iron slag forms at high temperatures ranging around 1300–1400 °C and typically required tall furnaces with powerful air supplies (Blomgren and Tholander, 1986). However, the furnaces found in Daye are notably short (0.5 m), and a plot of the slag composition in the FeO-Al_2O_3-SiO_2 phase equilibrium allows estimates that the slag was molten in the temperature range of 1100–1200 °C, as typical of bloomery systems (Fig. 13).

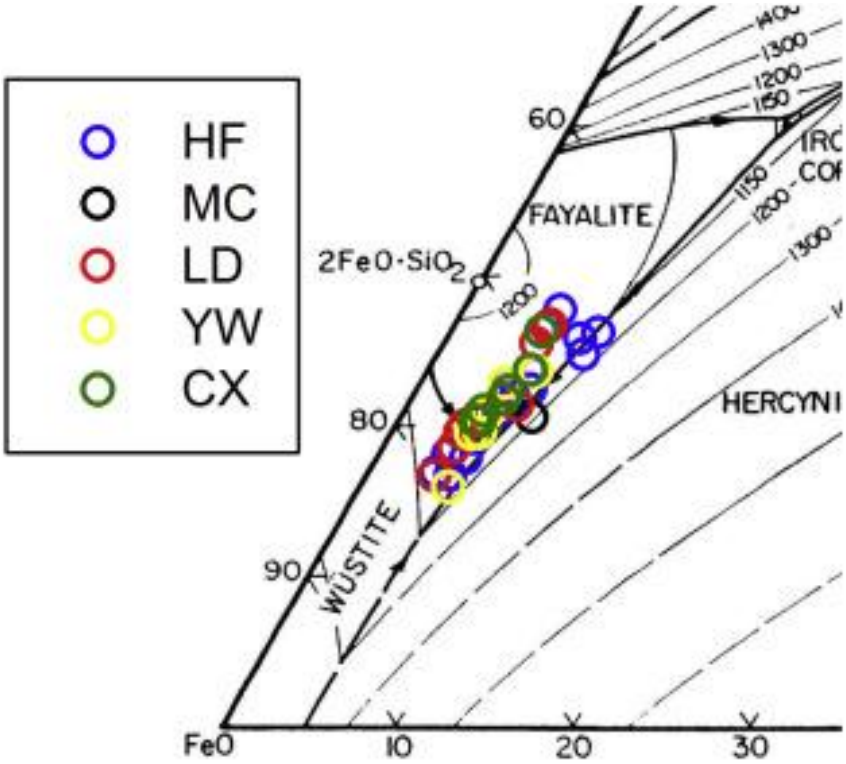

Fig. 13. Ternary system FeO-Al_2O_3-SiO_2 plotting all the Daye bloomery iron tap slag.

3.2 Reconstruction of the *châine opératoire*

The tap iron slag samples form a relatively tight cluster in the ternary diagram shown in Fig. 13, and they do not show differences by site; this provides a first indication that they derive from a broadly similar smelting procedure. The similarity among the by-products is observed in other parameters such as the analogous morphology of the slag; microstructure and mineralogy; bulk chemical composition; furnace typology and ceramic fabrics, and radiocarbon dates. Specifically, the tap slag assemblage presents a broad similarity in bulk composition that allows the recognition of a single chemical group across all the sites, which suggest that the different sites were using a similar smelting recipe employing the same raw materials (Fig. 11). To further investigate the homogeneity of the slag, a principal components analysis was carried

out including the major elements of the chemical composition (Fig. 14). The loading vectors show nicely the correlations among the four ceramic oxides (K_2O, Al_2O_3, SiO_2, TiO_2), negatively correlated to FeO. The PCA confirms the close similarities among the by-products regardless of the site, particularly clear in CX, LD, YW and HF, with the exception of the Cu-rich outlier YW4. The variation observed in MC is not really meaningful considering the small size of the sample (2 specimens). Overall, the PCA confirms the similarity of the by-products and supports the inference of a rather uniform technological process.

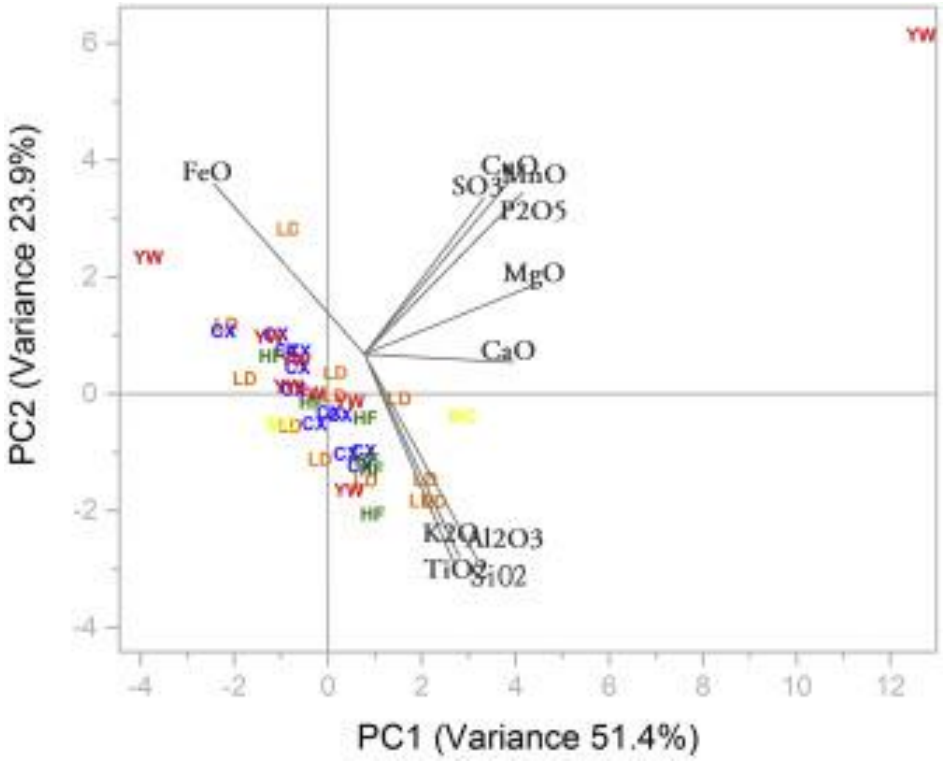

Fig. 14. PCA plot showing the variances in bulk composition of tap slag per site (first three components explain 74.1% of cumulative variance).

In spite of the range of sites, all the Daye ferrous slag is seemingly related to the same bloomery production process, and framed within the 1650–1800 CE bracket according to the radiocarbon dates available. The reduction of a rich-grade iron oxide ore took place in embanked furnaces built of clay operating under reducing conditions with temperatures typically ranging at least 1100–1200 °C (the melting point of the slag), generating fayalitic molten slag that was tapped out of the furnace, whereas solid ferritic iron metal coalesced into a bloom within it.

3.3 Mass balance calculation (MBC)

The cost of producing slag at relatively low temperatures, as was the case in Daye, was a loss of potentially reducible iron into the slag: this is because at temperatures around 1200 °C it is only possible to produce liquid slag if an iron-rich silicate melt is created, which means that a substantial quantity of the iron oxides present in the charge are not reduced but slagged. The loss of metal in slag was tolerable by ancient smelters if the ore grade was of 70–80% FeO (Rostoker and Bronson, 1990, 92; Buchwald, 2005, 93). Even though the analyses of the ore

fragments from Daye reveal that these range between 78 and 95% FeO content (Table 5), and are thus very suitable for bloomery smelting, the average FeO content in the tap slag is equally very high; a median of 72% FeO was sacrificed in the slag (Fig. 11).

In order to estimate the efficiency in the extraction of the iron metal from the ore, the output of metal was calculated following the MBC method proposed by Crew (2000). This model is based on the *'enrichment factor (EF)'* principle: as iron is removed from the system and reduced to metal, the remaining elements respectively increase in concentration, which allows an estimate of the yield of metal throughout this coefficient as calculated from the slag composition. All the calculations are based on the data from Yanwopu since this is the only site from where ore, furnace wall, slag and charcoal were recovered. The best-fit material solution contemplates the likely possibility of using blended ores with an average richness of 85% FeO, and estimates a yield of 24.5% Fe for slag that is made by 91% ore oxides, with a contribution of 8.1% clay and 0.9% fuel ash (Fig. 15). A first observation is that the efficiency in the reduction of metal in Daye is rather modest: this is illustrated through a comparison with similar calculations performed on data from other smelting sites from earlier chronologies across the world (Fig. 16).

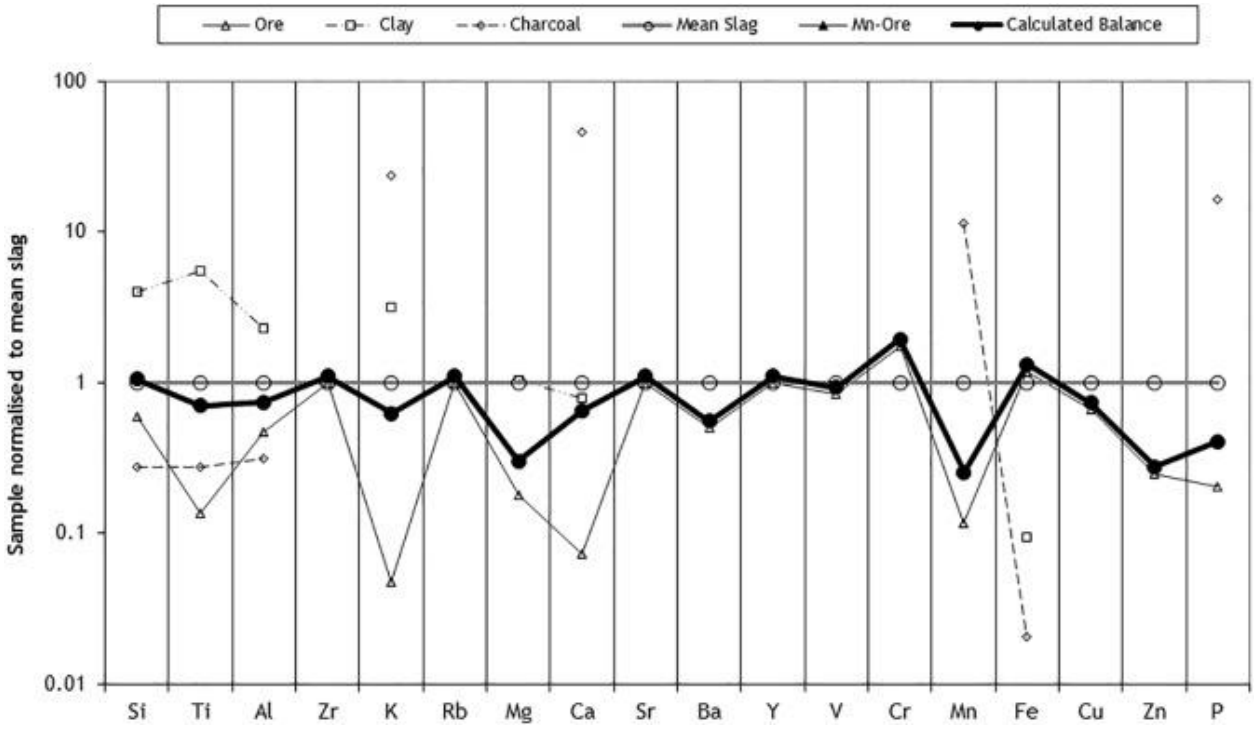

Fig. 15. Best-fit materials balance: EF = 1.21; 91.0% ore +8.1% clay +0.9% fuel ash = 24.6% iron yield.

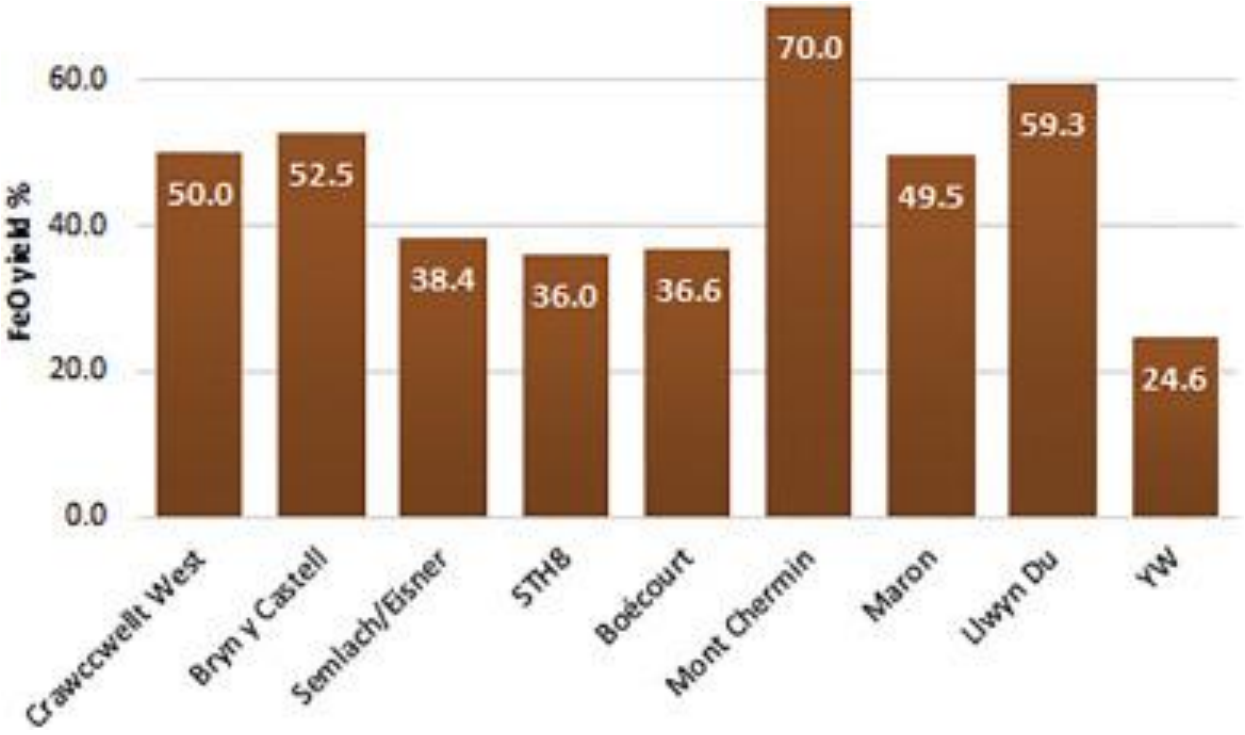

Fig. 16. Bart chart showing the estimated iron yield of several bloomery iron smelting sites in comparison to Daye (YW).

Crawcwellt West (UK), Iron Age; Bryn and Castell (UK), Late Iron Age to Roman; Semlach/Eisner (Austria), 100–400 CE; STH8 (Thailand), 200–500 CE; Boécourt (France), 400–700 CE; Mont Chemin (France), 400–700 CE; Maron (France); Llwyn Du (UK), 1300–1400 CE; Yanwopu (China), 1650–1800 CE. All data as provided by the corresponding authors using the same method of calculation (Crew et al., 2011) with the exception of Semlach/Eisner (Fillery-Travis, 2015) which uses a different method of calculation, Thomas & Young 1999, also based on the EF principle. STH8 from Venunan (2015), UK sites from Charlton (2006), and French sites from Crew et al. (2011).

3.4 Contribution of the furnace lining and technical shortcomings

As noted above, the main compounds in the composition of technical ceramics, slag and ore are iron oxide, silica and alumina, which typically make up around 95% of the composition. These are the main contributors in a relatively closed system: based on the slag analyses and MBC, no other material (e.g. silica-rich flux) was added to the furnace, and the estimated contribution of the fuel ash to the slag is minimal (0.9%). Considering the purity of the ore and its low silica content, the contribution of the furnace wall was essential for the formation of slag. In this vein, the paste preparation for the bloomery furnaces resulting in ceramics prone to interact chemically with the charge it is interpreted as an intentional practice to create a silica-rich slurry on the inner surface so that the ceramics could flux the smelt. This observation is coherent with the suggestion that each of the furnace structures in LD was only used for a short period of time before it needed repairs, and with the repeated relining evident in the archaeological remains, with an extreme case of 17 consecutive layers of relining preserved in a furnace (Hu et al., 2013, 294).

Similar solutions to the embanked furnaces found in Lidegui were widely in use in Eastern Europe during the Early Medieval period (Pleiner, 2000, 75–79). These ironworks were based on batteries of permanent furnaces, set alongside one another with their furnace arches all facing in the same direction. The shafts were cut out of the clay block and their front walls modelled in clay, thus the features were easy to repair by replacing the internal lining. According to Pleiner, a bloomery of 20 embanked furnaces would have a capacity of production of 6 or 7 t annually, based on reasonable estimates of a yield of 5 kg of iron per smelt and a total of sixty smelts per year (Pleiner, 2000, 76).

However, the LD embanked furnaces appear to be too small in comparison to European furnaces: the typical dimensions of the cylindrical shaft of European medieval embanked furnaces are 100–150 cm high and 22–35 cm in diameter (Pleiner, 2000, 75–79; Joosten, 2004, 13) whereas in LD the dimensions are 50 cm high for the funnel-shaped shaft, 35–60 cm diameter at the top and 20–36 cm at the bottom. These small dimensions constrained the capacity for large production.

Therefore, it is argued here that the low yield in Daye was mainly a consequence of two choices: 1) not controlling more effectively the charge composition by adding a silica-rich flux instead of relying exclusively in the contribution of the furnace walls; and 2) not building a taller furnace with more capacity to hold a larger charge and facilitate the circulation of reducing gases.

3.5. Rational economy: costs and benefits in the smelting operations

In sum, a significant amount of labour, time and resources was required to develop the volume of activities documented in Daye, yet the efficiency was low. For the sake of comparison, a single traditional Chinese ‘dwarf’ blast furnace in Dabieshan–a mountainous region close to Daye–was capable of producing 600–1200 kg of cast iron per day working for 6–7 days without requiring a repair, and it was easily handled by just 2–3 people (Wagner, 1997, 18) (Fig. 17). Charlton et al. (2010, 357) have hypothesised that bloomery slags with low fuel to ore ratios and chemistry close to the iron-rich eutectic, as is the case of the Daye slag (Fig. 13), ‘would be favoured in economies where there is little competition and the demand for iron is relatively low’. This could be a possible explanation for the choice of a low efficiency process in Daye.

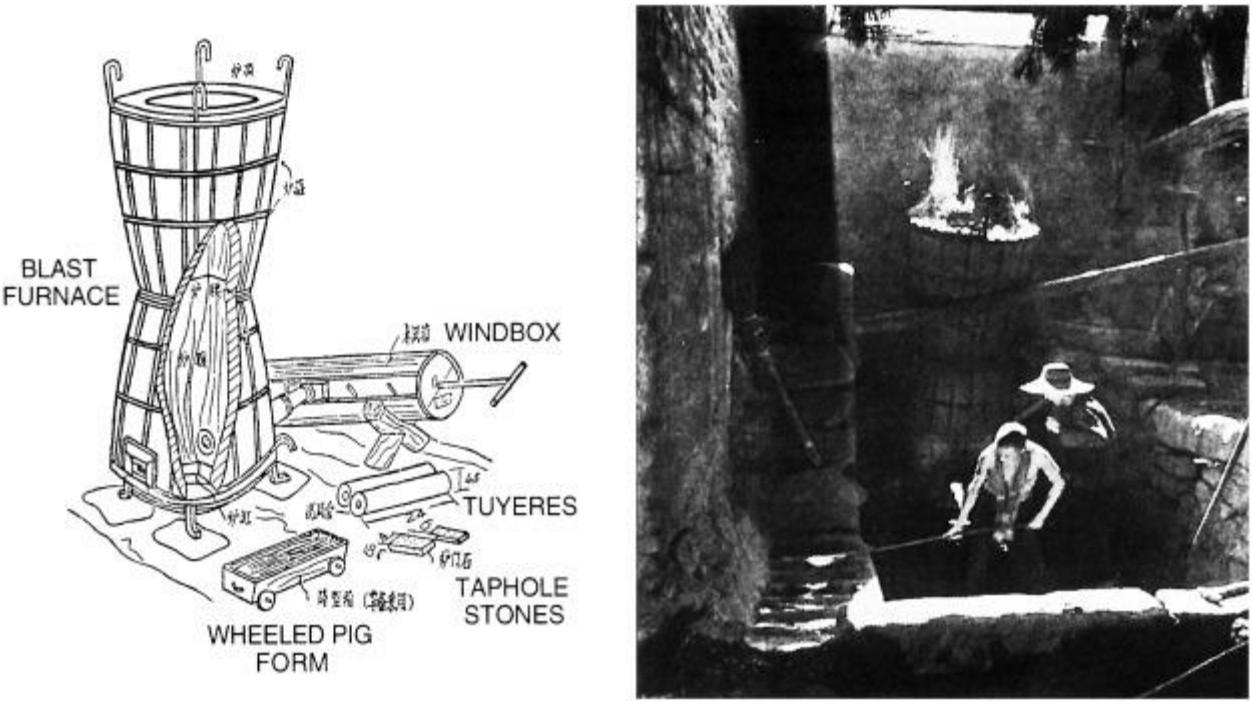

Fig. 17. Sketch of the Dabieshan small `dwarf' blast furnace as used in the Great Leap Forward period and picture of a blast furnace in operation in 1958.

Furnace is around 2.2 m high. From Wagner, 1997, Fig. 4, Fig. 6).

During the Qing Dynasty there was a generalised increase in the demand of iron that could not be satisfied by domestic production, to the point that China started to import raw iron from Western producers. This shortage was aggravated by a lack of an integrated and coherent system of communication and trading throughout the whole empire which inhibited a regular supply for long distance markets. Overall, transport was costly, unstable and extremely slow (Skinner, 1985; Wagner, 1997; Cao, 2012, 121–150), to the point that 'in more isolated regions, such as Dabieshan, transportation costs added so much to the cost of iron that it was economically rational to set up a small scale production for local needs in spite of its relative inefficiency' (Wagner, 2008, 6). Therefore, it is conceivable that communities in Daye resolved to produce their own iron. In this case, there would be no real market pressure since they were producing for a small market, likely the immediate local market, i.e. themselves.

The tentative scenario presented in this paper is that the smelters were low class unskilled commoners focused on the exploitation of a local resource, with little or no investment, as a solution for enlarging their income and balance the deficit of iron products. The undertaking of side activities by commoners to increase their income was normal within the context of economic recession during the 18th century in China, although the typical extra activities were textiles or profitable crops such as tea or tobacco (Rowe, 2009, 94). The small investment is evident in the digging of furnaces directly into the earth, thus saving the cost of building complex structures such as blast furnaces with multiple parts and different construction materials. Smelters could also make the charcoal themselves–the most expensive raw material–since they had access to forests. Finally, nodules of high grade iron ore can still be easily picked up from surface, suggesting that the ore was possibly the most accessible of the necessary raw materials. The tax burden relaxation policy to encourage small shareholders

focused on the exploitation of local sectors exerted by the Qing Dynasty also played to their benefit, since in exchange for the right to use the land's natural resources they most likely had to pay to the state with a small–if any–burden (Rowe, 2009, 91ff; Deng, 2015; Wu, 2015, 18ff). It is possible that Daye bloomery smelters operated outside the taxation issued to the iron sector, since the regulation applied to iron plants producing cast iron by blast furnaces whereas bloomery iron is not mentioned in the historical sources (Wagner, 1997; Li, 2009).

The hypothesis that the iron smelting sites in the Daye County were run by non-professional metalworkers would explain why the smelting process obtained a limited yield per smelt. The period of activity was likely short (1735–1800 following the most probable range measured by the radiocarbon dates, Fig. 6), and therefore not allowing a significant improvement of the technique via trial and error. It is also possible that smelters tried to compensate for the low iron yields per furnace by increasing the number of furnaces and bloomeries (Fig. 2), instead of through technical modification of the furnace design to optimise the output. This, once again, suggests that the smelters were not professional metalworkers.

This scenario would also explain the choice of iron production by the direct method instead of the more yield-efficient indirect method, since an important fact about indirect iron production is that 'it provides unusually large economies of scale' (Wagner, 2008, 6) intended for mass-production to supply large markets. The term rational economy is used here referring to the choice made by the producers of discarding the indirect method in favour of the direct method on the basis of a cost/benefit balance (Wagner, 2008, 6ff). The blast furnace technology would have rendered a considerable higher yield, yet they picked a production scale which filled their needs. In Daye, the rational economy is visible in the use of a method of production that allows non-professional metallurgists to reduce iron with limited knowledge, capital, and technological resources,

While the circumstances of commoners diversifying activities to complement their incomes is not a novelty–with many examples within China and beyond–a more unexpected finding of this research is the type of iron that was produced, i.e. bloomery iron, whose production was supposed to have ceased in China 2000 years earlier in favour of blast furnaces. The survival or resumption of bloomery iron in China therefore deserves further discussion.

3.6. Technological change and cultural tradition

The absence of bloomery iron in the archaeological record after the imperial monopoly of iron production in the year 117 BCE has been considered 'odd' by some scholars (e.g. Wagner, 2008, 246). However, the apparent absence of evidence for bloomery iron production would appear to confirm the first statement, and the few cases of bloomery iron documented have typically been explained as marginal productions in peripheral areas under the influence of the empire during early dynasties, when the state administration was not totally consolidated (e.g. Huang, 2013).

Technological change can be viewed as the result of the movement and transmission of information and culture traits, a process similar to the inheritance of genes in biological evolution, where the cultural traits include the materials required to construct a product, the production tools and facilities employed, the knowledge or practices required for production, and the ways in which final products are used (Lam, 2014). The sequences of changes result from rational choices where the technical means are selected in accordance with different social strategies, rules, and adaptations to variable conditions, and where different technological solutions can co-exist (Roux, 2008).

In the case of Daye, if the metallurgical tradition in the area was the production of cast iron, it is very hard to understand why unskilled non-professional metalworkers would have started to use a technology for which they had no previous knowledge, especially considering that the smelting of iron was presumably a means to complement their income, and thus experimenting with an unknown technology would seem an undesirable risk. Therefore, we are compelled to consider the possibility that bloomery technology was already known in Daye before the 18thcentury BC.

As a matter of fact, we propose here that there is additional evidence for bloomery iron production in Daye, but that this may have been misidentified in previous work. The excavation of Tonglüshan also revealed the presence of bowl furnaces related to iron production and dated to the Northern Song Dynasty (960–1127 CE) (Huangshi Municipal Museum, 1980; Wagner, 1986). As many as 17 bowl furnaces were excavated within a workshop of 320 m^2; these furnaces were small devices (around 37 cm of diameter) with one tuyere at the rear opposite the tap-hole, and the walls were relined with clay several times (Fig. 18). The associated debris is tap slag of fayalitic composition (65% FeO, 21% SiO_2). Having ruled out the production of copper, lead and silver, researchers suggested that these were by-products of fining furnaces used to decarburise cast iron. The main arguments raised to support this statement were that the slag was generated under oxidising conditions, contained some prills with high carbon content, and had a bulk iron content too high for it to be a cast iron smelting slag (Zhu and Zhang, 1986, 473). Nonetheless, there is no written or archaeological evidence of any production or decarburisation of cast iron in Daye and, more importantly and as acknowledged by the authors themselves, neither the high volume of slag nor the typology of the furnaces fit into the traditional fining furnaces known for the period (Zhu, 1986; Zhu and Zhang, 1986), i.e. large tall cupola furnaces (around 3 m high) or open-hearth fining devices that somewhat resemble a smith's forge (Wagner, 1997, 24).

Fig. 18. Remains of a bowl furnace of Northern Song Dynasty found in Tonglüshan with slag stuck to the tap-hole compared to furnace 12 of LD seen from the rear.

Tonglüshan picture from Huangshi Municipal Museum (1980, unpaged).

Furthermore, the characterisation of the slag provided is identical to typical bloomery iron slag as reported in this paper, with glassy matrix, fayalite laths, and few sub-angular iron particles that correspond to ferrite. The main exception is that the main free iron oxide is reported as magnetite rather than wüstite, although it is acknowledged that the latter is also regularly present in the slag (Zhu and Zhang, 1986, 471). In the micrographs of slag provided in the paper, the free iron oxides are systematically dendrites of globular shapes (Zhu and Zhang, 1986, Fig. 2, Fig. 3, Fig. 4, Fig. 5), different from the angular flakes that are typical of magnetite. In addition, since this is tap slag, it would not be surprising to find magnetite, particularly towards the surfaces of the slag, resulting from oxidation during cooling and hence not reflecting the furnace atmosphere. Therefore, it is our opinion that these slags were incorrectly interpreted as fining slag, perhaps based on the misidentification of wüstite as magnetite.

In stark contrast with these samples, fining slag typically presents a complex intergrowth of mineral phases in the matrix in which magnetite is frequently arranged as clusters; fayalite as large agglomerations of crystals; and also abundant crystals of hercynite, large grains of silica and iron sulphides (Killick and Gordon, 1987; Buchwald, 2003). Notably, the tap iron slag from the Song Dynasty found in Tonglüshan lacks of any of these diagnostic characteristics of fining slag whereas the characterisation fits comfortably into the description of bloomery slag. The presence of the liquid iron prills can be explained as the result of occasional conditions in which over-carburised iron is generated within the bloomery process.

Turning to the bowl furnace structures, these seem more appropriate to create a reducing atmosphere favourable for smelting rather than an oxidising one as expected for fining; the tuyere hole is placed at the bottom rear of the structure, while the blast of air in a refining device of these characteristics is supplied from the top. Notably, the small dimensions, shape of the chamber–a truncated cone–and the multiple relining of the bowl furnaces are evocative of those of the embanked furnaces of Lidegui, characterised above, and these are appropriate to create a reducing atmosphere (Fig. 18). Consequently, it may be appropriate to suggest that those or similar structures were the cultural trait that links the Song with the Qing smelters: both of them reducing iron in small funnel-shape devices without the addition of flux, but relying on the contribution of the furnace wall, which required frequent relining, as is evident in the furnaces of both chronologies.

Ironmaking ‘was not simply an economic or technical activity, it was a subculture in its own right, with its own traditions, prejudices and hierarchies’ (Hayman, 2005, 9). In this vein, it seems reasonable that if the Daye smelters did not adopt the cast iron technology, the reason must lie not only in the rational choice adapted to context but also in the weight of their own technological tradition: they did not venture to change a familiar model for a different one.

3.7. Economy of scale versus rational economy

Besides the cultural arguments and the reappraisal of comparative materials found in Daye, a further powerful reason to explain why Daye did not adopt blast furnaces is related to the model of production. The production of cast iron–even if using ‘simple’ dwarf type furnaces–

still requires a considerable set-up of technical facilities between blast furnaces, powerful air supply systems, and fining structures; and each of them constructed of different and specific materials. It also requires substantially more ore and fuel: for example, to produce 1 ton of cast iron in 24 h, the small Dabieshan furnace consumed around 1400 kg of ore and 2 to 7.5 t of charcoal (Wagner, 1997, 14ff), and further refining and casting actions are required to produce utensils. In comparison, a bloom of 13.5 kg can be obtained in 5 h using 91 kg of charcoal and 41 kg of ore (Sauder and Williams, 2002); the bloom is ready to be directly transformed into an iron bar and manufacturing artefacts. The bloomery case is much more readily accessible than the indirect method since it requires far less investment in facilities and procurement of raw materials, and has the advantage that it can be put into practice immediately. Moreover, mass-production is not necessarily an asset if the production largely overwhelms the demand and the producer has no means to manufacture or trade the surplus.

The production of cast iron allows mass-production and standardisation of products, which is consistent with the generally accepted technological history of China (e.g. Needham, 1958; Han and Ko, 2007). However, this is a large-scale model of production strongly constrained by the economic situation and highly dependent on infrastructures connecting producers and consumers. This sophisticated production model requires large investment, sophisticated facilities, technical knowledge, abundant workforce, good transportation, ample markets, and administrative regulation. All these conditions simultaneously are only possible under favourable political, economic and social circumstances. These requirements are severely affected during periods of crisis and instability e.g. recession, war, population decline, etc., which affect the capacity of production, frequency to reach the market, cost and consumption, etc. Therefore, this large-scale capital-intensive technology is a rigid model that can be very sensitive to system variations and requires stability to survive (Lin, 1995; Wagner, 1997, 76ff). The circumstances during the 18th century in China certainly did not favour this model since China suffered economic recession, investment in the metallurgical sector was virtually inexistent, transportation was deficient, and the initiatives or legislation by the administration were focused on tax collection (Rowe, 2009, 96ff; Deng, 2015; Wu, 2015, 18ff). Furthermore, iron making technology was not integrated into a cohesive technology, with at least four main areas using very different technologies: crucibles in Shanxi; large (9–10 m) blast furnaces in Sichuan; ‘dwarf’ furnaces (2–3 m) in Dabieshan; and both large and small (5–6 m) blast furnaces in Guangdong (Wagner, 1997).

Bloomery iron production, on the other hand, is flexible and more easily adaptable to circumstances. While the yield per smelt is considerably lower, it is also much more economically rational in some contexts, consuming considerably fewer natural resources, and it can satisfy local demand regardless of economic or political turbulence. As such, bloomery iron would seem a more suitable model of production in areas where production was not concentrated, there was lower demand of the standard products, or where communication routes were not fluid (Wagner, 2001). Given the delicate general economic situation in 18th century China, a model of production based on domestic-scale labour-intensive technology was the most logical solution.

4. Conclusion

This paper has documented the production of bloomery iron in five sites in Daye County (Hubei) during the middle Qing Dynasty. Based on current knowledge, this is an extraordinary

occurrence in China, since the very few archaeological examples of this type of production are chronologically framed in pre-imperial times. Received wisdom suggested a total predominance of cast iron and the disappearance of bloomery iron by the Han period, after the introduction of the state monopoly on iron production. This work has explored the widely accepted scenario of the almost inevitable abandonment of bloomery iron in favour of cast iron in the late 2ndcentury BC, concluding that this is not a solid hypothesis, and that its unquestioned acceptance may have led researchers to overlook or misidentify additional bloomery remains.

We discussed that a large-scale capital-intensive model of production such as that required for cast iron industries is fragile, due to its reliance on the economic, political and social situation, and that this is only operative if both infra- and superstructures (roads, ports, laws, prices, etc.) are functioning harmoniously. As a result, these favourable conditions indispensable to sustain the model are unlikely to survive unchanged for a period of 2000 years, and it is argued that these prerequisites were but rarely met in some areas of China during the 18th century.

Even though the smelting process in Daye can be regarded as inefficient in terms of metal yield, the cost/benefit balance is low, and therefore, low capital technologies for iron production on a domestic scale such as the embanked bloomery furnaces of Daye are indeed a major aspect of the technological progress, reflecting the rational technological choices made by the smelters. Based on a reappraisal of comparative material excavated in Tonglüshan, it appears that in Daye there was a technological tradition of bloomery iron smelting in existence at least since the 11th century AD. As such, this paper begins to reveal the existence of different regional technological traditions and variability in iron production, and seriously challenges the traditional model of ferrous metal production in China, implicitly taken as universal and immutable.

Acknowledgements

We would like to thank the many colleagues that made this research possible, most specially Chen Kunlong and Liu Siran from the Institute of Historical Metallurgy and Materials, University of Science and Technology Beijing (USTB北京科技大学), and all the members of the archaeological group of Daye city and Tonglüshan Ancient Metallurgy Museum, especially Chen Shuxiang and Qu Yi. In London, we thank the support of colleagues at the UCL Institute of Archaeology, in particular Tom Gregory (SEM technician) and Phillip Austin (archaeobotanist who identified species for radiocarbon). Many thanks to Mike Charlton in particular for his extraordinary enthusiasm, kindness and suggestions. We are also grateful to John Moffet, librarian at the Needham Institute in Cambridge, for his assistance. This paper is based on the PhD dissertation undertaken by David Larreina-Garcia at the UCL Institute of Archaeology, under the primary supervision of Marcos Martinón-Torres, carried out with the financial support of a UCL Impact Scholarship funded by UCL, the Institute for Archaeo-Metallurgical Studies (IAMS) and the Rio Tinto Group. Radiocarbon dates were obtained through the NERC/AHRC radiocarbon service (grant n° NF/2014/2/12). Finally, special thanks are due to Thilo Rehren, Myrto Georgakopoulou, and Jianjun Mei–second supervisor and examiners of the PhD, respectively–for their time and constructive reviews.

Research Data: See Supplementary Materials

Full results (normalised) of WD-XRF data for bloomery slag samples, and precision and accuracy values of the machines monitored using certified reference materials (CRMs)

References

C. Bai. **Baoji shi yi men cun M2 chutu chunqiu tie jian can kuai fenxi jianding baogao (Analytical report of the iron sword fragment unearthed from Tomb no.2 in Yimen, Baoji).** Wenwu, 9 (1994), pp. 82-85. (in Chinese).

S. Blomgren, E. Tholander. **Influence of the ore smelting course on the slag microestructures at early ironmaking, usable as identification basis for the furnace process employed.** Scand. J. Metall., 15 (1986), pp. 151-160.

V.F. Buchwald. **Bloomery Iron, Osmund Iron, Finned Iron and Puddled Iron.** L.C. Nørbach (Ed.), Prehistoric and Medieval Direct Iron Smelting in Scandinavia an Europe, Aarhus University Press, Aarhus (2003), pp. 171-176.

V.F. Buchwald. **Iron and steel in ancient times, Historisk-filosofiske Skrifter 29. Copenhagen: Det Kongelige Danske Videnskabernes Selskab.** (2005).

BUIST. **Yi xian yan xia dou 44 Hao muzang tieqi jin xiang kaocha chubu bao (preliminary metallographic analysis on the iron objects unearthed from the tomb 44 in Yi county).** Kaogu, 4 (1975), pp. 241-423. (in Chinese).

J. Cao. **Mint Metal Mining and Minting in Sichuan, 1700–1900: Effects on the Regional Economy and Society.** Doctoral Dissertation. Electronic publication by Tübingen University (2012).

M. Charlton. **Ironworking in Northwest Wales*: An* Evolution *analysis.*** University College London, UCL Institute of Archaeology, Doctoral Dissertation (2006).

M. Charlton, P. Crew, Rehren Th, S. Shennan. **Explaining the evolution of ironmaking recipes - an example from Northwest Wales.** J. Anthropol. Archaeol., 29 (2010), pp. 352-367.

J. Chen. **Zhongguo Gudai Jinshu Ye Zhu Wenming Xin Tan (Ancient China Metal Smelting and Casting Civilization).** Science Press, Beijing (2014). (in Chinese).

J. Chen, J. Yanh, B. Sun, Y. Pan. **Liang dai cun yizhi M27 chutu tong tie fuhe qi de zhizuo jishu (Manufacturing technique of the bronze-iron alloy artefact in M27 from Liangdai Village).** Science in China, 9 (2009), pp. 1574-1581. (in Chinese).

J. Chen, R. Mao, H. Wang, H. Chen, Y. Cie, Y. Qian. **Gansu lin tan mo gou si Wa wenhua muzang chutu tieqi yu zhongguo ye tie jishu qiyuan (Iron objects unearthed from a Siwa Culture tomb in Lintan (Gansu) and the origin of Chinese iron metallurgy).** Wenwu, 8 (2012), pp. 45-53. (in Chinese).

T. Chuenpee, K. Won-In, S. Natapintu, L. Takashima. **Archaeometallurgical Studies of Ancient Iron Smelting Slags from Ban Khao Din Tai Archaeological Site, Northeastern Thailand.** J. Appl. Sci., 14 (9) (2014), pp. 938-943.

Changsha Railway Construction, Excavation Team. **Zhangsha xin faxian chunqiu wanqi de gang jian he tieqi (Iron swords and objects from the late Spring and Autumn period found in Changsha).** Wenwu, 10 (1978), pp. 44-48. (in Chinese).

P. Crew, M. Charlton, P. Dillmann, C. Salter, E. Truffaut. **Cast iron from a bloomery furnace, in *The Archaeometallurgy of Iron: recent developments in archaeological and scientific research.*** Praha: Institute of Archaeology of the ASCR (2011), pp. 239-316.

K. Deng. **China's Population expansion and its causes during the Qing Period, 1644–1911.** Econ. Hist. Work. Pap., 219 (2015), pp. 1-55.

N.L. Erb-Satullo, J.T. Walton. **Iron and copper production at Iron Age Ashkelon: Implications for the organization of Levantine metal production.** *Journal of Archaeological Science: Reports*. Elsevier, 15 (January) (2017), pp. 8-19.

A. Espelund. **Bloomery ironmaking during the Roman period in mid-Norway.** Hist. Metall., 48 (1) (2015), pp. 16-24.

R. Fillery-Travis. **Iron production in the Western Roman Empire*: A diachronic study of* Technology *and* Society *based on two archaeological sites.*** University College London, UCL Institute of Archaeology, Doctoral Dissertation (2015).

I. Freestone. **Refractory materials and their procurement.** A. Hauptmann, E. Pernicka, G.A. Wagner (Eds.), *Old World Archaeometallurgy – Archäometallurgie der alten Welt. Der Anschnitt, Beiheft 7.* Bochum: Deutsches Bergbau-Museum (1986), pp. 155-162.

P.J. Golas. ***Science and Civilisation in China, Part XIII: Mining*. Cambridge.** Cambridge University Press (1999).

R. Han. **Iron and steel making and it's features in ancient China.** Bull. Met. Mus., 30 (1998), pp. 23-37.

R. Han, T. Ko. **Zhongguo Kexue Jishu Shi Kuang Ye Juan (a History of Science and Technology in China: Mining and Metallurgy).** Science Press, Beijing (2007). (in Chinese).

R. Hayman. **Ironmaking : The History and Archaeology of the Iron Industry.** Tempus, Stroud (2005).

X. Hu, Y. Qu, C. Han, G. Wei, Y. Qin. **The Analysis of the Middle Qing Dynasty Iron Smelting Furnace at Hualushan, Lidegui Village in Hubei Province, in Tonglushan Gu Tong Kuang Yizhi Kaogu Faxian Yu Yanjiu (*The Discovery and Study of the Tonglushan Ancient Copper Mining and Smelting Site).*** Science Press, Beijing (2013), pp. 294-306. (in Chinese).

J. Hua. **The Mass production of Iron Castings in Ancient China.** Sci. Am., 248 (1) (1983), pp. 121-129.

Q. Huang. **Shisi-Shiqi Shiji Zhongguo Gangtie Shengchan Shi (*Chinese iron and steel production from 14th to 17th centuries).*** Zhongzhou Ancient Books Publishing House (1989). (in Chinese).

Huang Q. (2013) Guangxi Guigang Diqu Gudai Ye Tie Yizhi Diaocha Yu Luzha Yanjiu (Studies on the Ancient Iron Smelting Sites and Slag in Guigang District of Guangxi). Guangxi: Lijiang Publishing House (in Chinese).

Q. Huang, Y. Li. **Preliminiary Studies on Western Han Dynasty Iron Smelting Sites and Slag Found in Pignan County, Guangxi Province, China.** J. Humphris, T. Rehren (Eds.), The World of Iron, Archetype, London (2013), pp. 333-342.

Hubei Provincial Bureau of Cultural Heritage. **Zhongguo Wenwu Ditu Ji: Hubei Fence Xia Ce (Atlas of Chinese Cultural Heritage: Hubei).** Xi'an : Xi'an Atlas Press (2002).

T. Jiang. **Sanmenxia Guoguo Mu (Guoguo Cemetery in Sanmenxia). Beijing.** Cult. Relics Publ. House (1999). (in Chinese).

I. Joosten. **Technology of Early Historical Iron Production in the Netherlands.** Institute for Geo- and Bioarchaeology, Vrije Universiteit, Amsterdam (2004).

D. Killick, R.B. Gordon. **Microstructures of puddling slags from Fontley, England and Roxbury, Connecticut, USA, *Journal of Historical Metallurgy.*** Society, 21 (1) (1987), pp. 28-36.

W. Lam. **Everything old is new again? Rethinking the transition to cast Iron Production in the Central Plains of China.** J. Anthropol. Res., 70 (2014), pp. 511-542.

D. Larreina-Garcia. **Copper and bloomery iron smelting in Central China: Technological traditions in the Daye County (Hubei).** University College London, UCL Institute of Archaeology, Doctoral Dissertation (2017).

X. Li. **Mingshi Shi Huo Zhi Jiaozhu (Food, Spirits and Commodities during the Ming Dynasty).** Zhonghua Book Company, Zhengzhou (1982). (in Chinese).

J. Li. **The excavation and study of iron-smelting ruins in the Warring States period in Henan province.** China, *Bull. Met. Mus.*, 27 (1997), pp. 26-45.

H. Li. **Qian Qing zhongguo shehui ye tieye (Former Qing Society of Chinese Iron and Steel Industry).** J. Changzhou University (Social Sciences Edition), 10 (2) (2009), pp. 59-62. (in Chinese).

J.Y. Lin. **The Needham puzzle: why the Industrial Revolution did not originate in China.** Econ. Dev. Cult. Chang., 43 (2) (1995), pp. 269-292.

Y. Liu. **Shanxi lintong xin feng mudi chutu jinshu qi de kexue fenxi (A scientific study of metal objects unearthed from the Xinfeng cemetery in Lintong, Shaanxi Province).** Institute of Metallurgy and Materials University of Science and Technology Beijing (2016).

D. Liu, Y. Zhu. **Gansu lingtai xian jing jia zhuang chunqiu mu (a tomb dated to Spring-Autumn period in Jingjiazhuang, Lingtai, Gansu province).** Kaogu, 4 (1981), pp. 298-301. (in Chinese).

H. Liu, W. Qian, J. Chen, Y. Li, Y. Guo, N. Liu. **A preliminary study of furnace materials from Shuiquangou iron smelting site of Liao and Jin period in Beijing.** ISIJ Int., 54 (5) (2014), pp. 1159-1166.

F. Luo, K. Han. **Ningxia Guyuan jinnian faxian de beifang xa qingtongqi (Discoveries of northern bronzeware in Guyuan, Ningxia).** Kaogu, 5 (1990), pp. 403-418.

B. Maldonado, T. Rehren. **Early copper smelting at Itziparátzico, Mexico.** J. Archaeol. Sci., 36 (2009), pp. 1998-2006.

D. Miller, D. Killick. **Slag identification at southern african archaeological sites.** J. African Archaeology, 2 (1) (2004), pp. 23-47.

Nanjing Museum. **Jiangsu liuhe cheng qiao er Hao dongzhou mu (Tomb 2 from the East-Zhou period in Liuhe Chengqiao, Jiangsu).** Kaogu, 2 (1974), pp. 116-120.

Shandong Museum. **Linzi lang jia zhuang yi hao dongzhou xun ren mu (Tomb with human sacrifice in Langjia Village, Linzi).** Acta Archaeol. Sin., 1 (1977), pp. 73-104.

Huangshi Municipal Museum. **Tonglüshan (Mt. Verdigris Daye)- a Pearl among Ancient Mines.** Cultural Relics Publishing House, Beijing (1980). (Unpaged book).

Huangshi Municipal Museum. **Tonglushan gu kuang ye yizhi (Ancient mining and smelting site at Tonglüshan).** Cultural relics Publishing House, Beijing (1999). (in Chinese).

J. Needham. **The Development of Iron and Steel Technology in China.** Newcomen Society, Cambridge (1958).

R. Pleiner. **Iron in Archaeology: The European Bloomery Smelters.** Archeologigky Ustav Avcr, Prague (2000).

T. Rehren, M. Ganzelewski. **Early blast furnace and finery slags from the Jubach, Germany.** G. Magnusson (Ed.), The importance of ironmaking, Technological innovation and social change (1995), pp. 172-179. (Stockholm).

W. Rostoker, B. Bronson. **Pre-Industrial Iron: Its Technology and Ethnology, Archaeomaterials Monograph No. 1. Philadelphia.** University Press, Pennsylvania (1990).

V. Roux. **Evolutionary Trajectories of Technological Traits and Cultural Transmission.** M.T. Stark, L. Horne, B.J. B (Eds.), Cultural Transmission and Material Culture: Breaking Down Boundaries, University of Arizona Press, Tucson (2008), pp. 82-105.

T.W. Rowe. ***China's last empire, the Great Qing*.** Massachusetts: Belknap Press of Harvard University Press, London (2009).

L. Sauder, S. Williams. **A practical treatise on the smelting and smithing of bloomery iron.** Hist. Metall., 36 (2) (2002), pp. 122-131.

V. Serneels, S. Perret. **Quantification of smithing activities based on the investigation of slag and other material remains, in *Archaoeometallurgy in Europe*.** Milano: Associacione Italiana di Metallurgia (2003), pp. 469-478.

Q. Sima. ***Shiji (The Scribe's Records)*. Beijing: Zhonghua Book Company (Historical record written in 1st century BC, republished in 1959).** (1959). (in Chinese).

G.W. Skinner. **The Structure of Chinese history.** J. Asian Stud., 44 (2) (1985), pp. 271-292.

W. Sun. **Lintong Xin Feng Qin Mu Yanjiu (Study of the Xinfeng Cemetery in Lintong).** Northwest University (2009). (in Chinese).

G.R. Thomas, T.P. Young. **The determination of bloomery furnace mass balance and efficiency.** A.M. Pollard (Ed.), Geoarchaeology: exploration, environments, resources, 165, Special Publications, Geological Society, London (1999), pp. 155-164, DOI: 10.1144/GSL.SP.1999.165.01.12.

P. Venunan. **An archaeometallurgical study of iron production in Ban Kruat, lower Northeast Thailand: Technology and Soc. Dev. from the Iron Age to the imperial Angkorian Khmer period (fifth century BC – fifteenth century AD).** University College London, UCL Institute of Archaeology, Doctoral Dissertation (2015).

D.B. Wagner. **Ancient Chinese copper smelting, sixth century BC: recent excavation and simulation experiments.** J. Hist. Metall. Soc., 20 (1) (1986), pp. 1-16.

Wagner D. B. **The traditional Chinese iron industry and its modern fate**. Nordic Institute of Asian Studies 32 (1997). Richmond: Curzon.

D.B. Wagner. ***The state and the iron industry in Han China*. Copenhagen: Nordic Institute of Asian Studies.** (2001).

D.B. Wagner. ***Science and Civilisation in China, Part XI: Ferrous metallurgy*. Editado Por J. Needham.** Cambridge University Press (2008).

J.R. White. **Historic blast furnace slag: Archaeological and metallurgical analysis.** Journal of Historical Metallurgy Society, 14 (1980), pp. 55-64.

Wu S. X. **Empires of Coal*: Fueling China's Entry into the Modern World Order, 1860–1920.*** Stanford, California: Stanford University Press (2015).

C. Xu, J. Li, Z. Wei, X. Han, S. Yan. **Ningxia guyuan yang lang qingtong wenhua mudi (Bronze culture cemetery in Yanglang, Guyuan, Ningxia).** Acta Archaeol. Sin., 1 (1993), pp. 13-56. (in Chinese).

K. Yang. ***Zhongguo gudai ye tie jishu fazhan shi (History of the development of iron metallurgy in China)*.** Shanghai: Shanghai people's Publishing House (1982). (in Chinese).

S. Zhu. **Ancient metallurgy of non-ferrous metals in China.** Bull. Met. Mus., 11 (1986), pp. 1-13.

S. Zhu, W. Zhang. **A study of the song period metallurgical furnaces at Tonglüshan in Daye County, Hubei (in Chinese).** Kaogu, 1 (1986), pp. 469-476.

H. Zou. **Tiamma-Qucun (Tianma Village).** Science Press, Beijing (2000). (in Chinese).

Supplementary materials I, Normalised WD-XRF data for bloomery slag samples

(as given by Department of Geociences, University of Fribourg)

Sample	Na_2O	MgO	Al_2O_3	SiO_2	P_2O_5	SO_3	K_2O	CaO	TiO_2	MnO	Fe_2O_3
CX1	0.11	0.35	3.21	16.28	0.09	0.03	0.41	0.43	0.14	0.11	78.60
CX2	0.10	0.46	4.94	21.24	0.20	0.07	0.68	0.64	0.21	0.12	71.01
CX3	0.14	0.53	4.37	23.48	0.17	0.06	0.62	1.06	0.22	0.14	68.99
CX4	0.16	0.42	4.44	19.53	0.13	0.07	0.58	0.64	0.22	0.14	73.49
CX5	0.10	0.46	3.74	18.83	0.15	0.06	0.56	0.54	0.17	0.18	75.02
CX6	0.09	0.45	3.62	17.48	0.17	0.06	0.49	0.51	0.15	0.15	76.64
CX7	0.09	0.46	3.62	18.22	0.15	0.07	0.51	0.57	0.16	0.16	75.79
CX8	0.13	0.46	4.42	19.96	0.19	0.07	0.66	0.68	0.19	0.16	72.84
CX9	0.11	0.50	4.53	20.75	0.19	0.08	0.61	0.59	0.20	0.17	72.08
CX10	0.08	0.43	3.82	18.16	0.16	0.06	0.63	0.66	0.20	0.11	75.48
CX12	0.14	0.55	4.16	23.84	0.20	0.08	0.66	0.75	0.21	0.11	69.07
CX13	0.17	0.49	3.75	18.65	0.20	0.08	0.50	0.63	0.16	0.12	75.03
HF8	0.09	0.52	4.94	19.47	0.22	0.08	0.78	1.35	0.19	0.19	71.89
HF9	0.08	0.39	4.58	18.82	0.15	0.07	0.70	0.68	0.17	0.14	73.92
HF14	0.17	0.53	5.53	20.05	0.29	0.06	0.98	1.00	0.18	0.12	70.89
HF18	0.10	0.52	4.26	16.06	0.13	0.05	0.66	0.64	0.13	0.11	77.18
HF21	0.03	0.25	3.10	15.14	0.35	0.18	0.52	0.62	0.11	0.12	79.44
HF22	0.04	0.40	3.07	15.05	0.37	0.07	0.75	1.32	0.11	0.14	78.48
HF23	0.19	0.54	4.38	19.56	0.29	0.09	0.54	0.59	0.14	0.12	73.35
HF24	0.06	0.40	2.95	13.24	0.21	0.07	0.58	0.77	0.12	0.12	81.29
HF25	0.11	0.48	4.82	24.74	0.16	0.05	1.00	0.84	0.20	0.13	67.20
LD1	0.24	0.26	3.52	18.49	0.15	0.05	0.94	0.94	0.21	0.12	74.89
LD2	0.22	0.27	3.13	14.90	0.16	0.06	0.77	0.53	0.13	0.08	79.60
LD3	0.14	0.44	3.16	17.60	0.33	0.09	0.84	1.69	0.22	0.11	75.18
LD4	0.18	0.43	3.47	18.95	0.25	0.08	1.15	1.38	0.16	0.15	73.61
LD5	0.27	0.54	4.52	23.39	0.28	0.07	1.23	2.29	0.21	0.13	66.84
LD6	0.26	0.52	4.36	22.18	0.27	0.10	1.29	2.57	0.21	0.14	67.88
LD7	0.28	0.56	4.45	23.16	0.28	0.09	1.28	2.50	0.22	0.14	66.82
LD8	0.26	0.43	5.22	18.92	0.19	0.06	1.09	1.14	0.24	0.21	72.03
LD9	0.26	0.23	3.19	17.47	0.15	0.04	0.68	0.75	0.17	0.10	76.77
Sample	**Na_2O**	**MgO**	**Al_2O_3**	**SiO_2**	**P_2O_5**	**SO_3**	**K_2O**	**CaO**	**TiO_2**	**MnO**	**Fe_2O_3**
LD11	0.30	0.58	3.18	15.99	0.42	0.05	1.01	3.14	0.14	0.12	74.84

LD12	0.13	0.52	3.29	18.87	0.39	0.12	1.12	2.41	0.24	0.13	72.54
LD13	0.25	0.32	3.63	18.32	0.17	0.05	0.88	0.91	0.30	0.16	74.71
LD14	0.04	0.46	3.67	14.69	0.23	0.12	0.26	0.34	0.13	0.26	79.56
MC1	0.25	0.24	4.11	18.27	0.12	0.05	0.77	0.76	0.19	0.11	74.88
MC6	0.31	0.84	6.19	17.78	0.33	0.06	0.99	2.82	0.17	0.28	69.89
MC12	0.26	0.64	7.04	25.46	0.23	0.06	1.45	1.51	0.28	0.14	62.65
MC18	0.86	0.50	4.60	24.13	0.28	0.03	0.45	3.13	0.16	0.03	65.54
YW1	0.14	0.54	3.98	20.21	0.23	0.07	0.59	1.63	0.20	0.13	72.02
YW2	0.10	0.47	4.20	17.49	0.15	0.06	0.52	0.62	0.19	0.09	75.86
YW3	0.08	0.47	3.80	17.46	0.14	0.08	0.50	0.52	0.20	0.12	76.43
YW4	0.05	1.57	4.49	23.08	1.94	0.23	0.78	4.54	0.21	0.88	61.21
YW5	0.11	0.43	4.01	18.44	0.24	0.06	0.63	1.30	0.18	0.09	74.28
YW6	0.12	0.46	5.30	21.15	0.16	0.06	0.87	0.62	0.22	0.10	70.73
YW7	0.11	0.46	4.17	14.20	0.14	0.06	0.71	0.88	0.14	0.10	78.86

Sample	CuO	Cl	V_2O_5	Cr_2O_3	Co_3O_4	NiO	ZnO	Ga_2O_3	GeO_2	As_2O_3	Br	Rb_2O	SrO	Y_2O_3	ZrO_2	Nb_2O_5	MoO_3	Ag_2O	CdO	In_2O_3
CX1	81	bdl	712	141	499	bdl	25	17	11	bdl	bdl	23	22	13	94	bdl	131	42	49	bdl
CX2	61	14	1160	155	448	bdl	105	9	bdl	bdl	bdl	32	48	13	134	2	204	54	48	17
CX3	10	bdl	781	171	427	bdl	18	18	bdl	bdl	bdl	28	47	11	145	bdl	157	42	11	1
CX4	bdl	bdl	595	151	277	bdl	12	57	bdl	bdl	bdl	30	42	7	126	1	182	59	47	63
CX5	bdl	bdl	693	146	238	bdl	21	17	11	bdl	bdl	37	35	8	118	bdl	130	23	18	11
CX6	bdl	bdl	798	131	286	bdl	bdl	37	15	bdl	bdl	33	34	15	91	bdl	125	27	25	bdl
CX7	bdl	bdl	732	79	444	bdl	16	41	bdl	bdl	bdl	29	42	10	98	bdl	134	41	31	18
CX8	bdl	10	871	199	288	bdl	10	16	bdl	bdl	bdl	28	41	13	126	bdl	110	40	55	bdl
CX9	14	38	721	128	462	bdl	12	34	9	bdl	bdl	38	40	11	120	bdl	148	46	46	17
CX10	bdl	bdl	1150	138	233	bdl	bdl	16	bdl	bdl	bdl	34	44	8	127	2	143	62	54	13
CX12	64	118	463	157	420	bdl	78	bdl	bdl	bdl	bdl	36	39	11	138	3	138	45	43	10
CX13	10	94	769	171	482	bdl	22	21	bdl	bdl	bdl	25	28	2	87	bdl	163	53	24	3
HF8	18	32	689	222	503	bdl	14	10	bdl	bdl	bdl	36	82	5	114	1	155	55	29	bdl
HF9	89	bdl	579	234	474	bdl	95	1	bdl	bdl	bdl	33	48	12	103	bdl	152	25	9	1
HF14	91	38	224	132	461	bdl	109	bdl	9	bdl	2	35	44	bdl	97	bdl	94	28	bdl	bdl
HF18	bdl	21	457	104	461	bdl	19	22	15	bdl	bdl	28	44	2	80	bdl	164	37	36	bdl
HF21	3	57	183	40	338	138	3	bdl	bdl	212	bdl	28	23	bdl	73	bdl	155	58	40	3
HF22	5	61	186	64	485	bdl	bdl	23	bdl	bdl	bdl	27	69	5	78	4	180	47	52	bdl
HF23	5	141	576	142	500	bdl	36	9	13	bdl	bdl	26	34	7	88	bdl	169	26	3	11
HF24	bdl	185	610	81	248	bdl	13	22	bdl	43	bdl	30	36	6	70	bdl	175	47	5	bdl
Sample	**CuO**	**Cl**	**V_2O_5**	**Cr_2O_3**	**Co_3O_4**	**NiO**	**ZnO**	**Ga_2O_3**	**GeO_2**	**As_2O_3**	**Br**	**Rb_2O**	**SrO**	**Y_2O_3**	**ZrO_2**	**Nb_2O_5**	**MoO_3**	**Ag_2O**	**CdO**	**In_2O_3**

HF25	68	39	885	128	491	bdl	93	16	bdl	bdl	bdl	50	50	7	100	bdl	129	27	25	bdl
LD1	bdl	bdl	462	103	458	bdl	54	bdl	bdl	bdl	bdl	32	72	bdl	162	bdl	157	44	13	bdl
LD2	bdl	bdl	592	68	419	bdl	41	19	bdl	bdl	bdl	20	28	bdl	63	bdl	124	42	21	bdl
LD3	bdl	30	559	56	481	bdl	bdl	19	14	bdl	bdl	32	90	13	78	bdl	115	47	42	bdl
LD4	bdl	bdl	470	87	356	bdl	33	29	bdl	bdl	bdl	37	82	17	111	bdl	160	47	15	bdl
LD5	95	bdl	452	119	485	bdl	77	bdl	bdl	bdl	bdl	36	96	bdl	165	bdl	172	16	bdl	bdl
LD6	89	bdl	425	85	490	bdl	87	11	bdl	bdl	bdl	33	98	13	171	bdl	140	43	36	bdl
LD7	29	bdl	461	119	476	bdl	bdl	23	bdl	bdl	bdl	37	105	14	173	bdl	156	55	44	bdl
LD8	16	bdl	746	87	485	bdl	29	45	bdl	bdl	bdl	42	77	14	140	bdl	108	50	56	bdl
LD9	bdl	59	396	63	479	bdl	29	43	bdl	bdl	bdl	34	39	bdl	92	bdl	176	27	79	bdl
LD11	136	bdl	266	44	479	bdl	75	42	bdl	bdl	bdl	30	224	bdl	78	bdl	111	34	21	bdl
LD12	78	bdl	668	72	435	bdl	88	15	9	bdl	bdl	44	128	11	84	1	123	61	35	29
LD13	bdl	23	1260	108	429	bdl	14	21	3	bdl	bdl	34	62	11	115	bdl	179	29	72	12
LD14	318	167	271	146	518	bdl	48	8	bdl	5	bdl	14	17	2	49	bdl	161	39	16	bdl
MC1	bdl	28	804	133	432	bdl	11	31	bdl	bdl	bdl	27	41	5	117	bdl	185	41	49	bdl
MC6	536	116	443	164	478	bdl	26	33	bdl	bdl	2	39	166	6	79	bdl	147	51	27	bdl
MC12	67	bdl	970	181	425	bdl	77	10	bdl	bdl	bdl	49	60	12	150	bdl	130	61	48	21
MC18	23	24	1430	262	482	bdl	1	25	bdl	bdl	bdl	29	177	10	21	bdl	120	47	32	bdl
YW1	81	44	474	268	466	bdl	104	2	5	bdl	bdl	35	61	bdl	109	4	126	45	32	bdl
YW2	61	34	508	272	466	bdl	87	31	bdl	bdl	bdl	32	48	5	117	3	139	66	49	bdl
YW3	107	20	210	128	487	bdl	93	bdl	bdl	bdl	bdl	30	33	5	126	bdl	118	48	46	16
YW4	5260	bdl	295	165	354	588	1480	35	bdl	bdl	bdl	bdl	19	332	5	109	bdl	722	26	bdl
Sample	**CuO**	**Cl**	**V_2O_5**	**Cr_2O_3**	**Co_3O_4**	**NiO**	**ZnO**	**Ga_2O_3**	**GeO_2**	**As_2O_3**	**Br**	**Rb_2O**	**SrO**	**Y_2O_3**	**ZrO_2**	**Nb_2O_5**	**MoO_3**	**Ag_2O**	**CdO**	**In_2O_3**

YW5	bdl	bdl	536	243	345	bdl	51	45	bdl	bdl	bdl	28	62	2	99	bdl	164	29	86	3
YW6	97	bdl	406	168	449	bdl	85	6	11	bdl	bdl	44	41	11	124	bdl	136	39	14	4
YW7	36	bdl	483	107	487	bdl	16	9	6	bdl	2	39	37	3	80	bdl	158	24	14	bdl

Sample	**SnO_2**	**Sb_2O_3**	**TeO_2**	**Cs_2O**	**BaO**	**La_2O_3**	**CeO_2**	**Nd_2O_3**	**HfO_2**	**Ta_2O_5**	**WO_3**	**PtO_2**	**Au**	**HgO**	**PbO**	**Bi_2O_3**	**ThO_2**
CX1	bdl	bdl	bdl	bdl	152	39	68	bdl	55	39	184	bdl	bdl	bdl	bdl	bdl	bdl
CX2	bdl	bdl	bdl	10	176	64	80	22	bdl	141	185	8	bdl	21	bdl	bdl	bdl
CX3	bdl	bdl	bdl	4	173	43	bdl	bdl	bdl	14	114	3	bdl	11	5	3	bdl
CX4	bdl	4	bdl	bdl	127	58	9	bdl	55	bdl	88	55	18	2	2	bdl	bdl
CX5	bdl	bdl	bdl	bdl	158	92	64	bdl	bdl	bdl	72	16	5	10	bdl	7	bdl
CX6	bdl	bdl	bdl	bdl	97	68	bdl	bdl	46	26	79	bdl	3	3	bdl	bdl	bdl
CX7	bdl	bdl	bdl	bdl	85	41	bdl	bdl	127	19	bdl	45	22	19	bdl	bdl	bdl
CX8	bdl	bdl	bdl	1	125	105	257	133	bdl	bdl	13	bdl	bdl	bdl	7	bdl	bdl
CX9	bdl	bdl	bdl	bdl	149	44	64	10	bdl	17	87	15	13	5	bdl	bdl	bdl
CX10	bdl	bdl	bdl	11	133	bdl	27	bdl	44	15	47	bdl	19	5	5	bdl	bdl
CX12	bdl	bdl	bdl	bdl	89	86	164	36	bdl	120	184	bdl	bdl	3	bdl	bdl	bdl
CX13	bdl	8	bdl	16	124	95	bdl	bdl	12	48	103	bdl	bdl	bdl	bdl	bdl	bdl
HF8	bdl	bdl	bdl	bdl	181	94	169	89	51	76	229	bdl	21	bdl	bdl	bdl	bdl
HF9	bdl	bdl	bdl	bdl	138	56	221	74	65	130	283	bdl	bdl	bdl	9	bdl	bdl
HF14	bdl	bdl	bdl	bdl	93	7	85	bdl	bdl	193	226	bdl	bdl	bdl	bdl	4	bdl
Sample	**SnO_2**	**Sb_2O_3**	**TeO_2**	**Cs_2O**	**BaO**	**La_2O_3**	**CeO_2**	**Nd_2O_3**	**HfO_2**	**Ta_2O_5**	**WO_3**	**PtO_2**	**Au**	**HgO**	**PbO**	**Bi_2O_3**	**ThO_2**

HF18	1	bdl	bdl	bdl	62	18	157	17	bdl	33	29	11	7	bdl	2	9	bdl
HF21	bdl	bdl	bdl	27	151	22	16	4	bdl	bdl	bdl	bdl	bdl	bdl	5	13	bdl
HF22	bdl	bdl	bdl	bdl	300	3	72	bdl	142	bdl	bdl	26	21	13	bdl	bdl	bdl
HF23	bdl	bdl	bdl	bdl	118	75	66	32	bdl	68	66	3	bdl	21	bdl	bdl	bdl
HF24	bdl	bdl	20	47	145	80	bdl	bdl	bdl	bdl	bdl	bdl	8	15	bdl	12	bdl
HF25	bdl	bdl	bdl	6	149	73	bdl	bdl	bdl	133	282	bdl	bdl	bdl	3	bdl	bdl
LD1	bdl	bdl	bdl	bdl	217	21	67	bdl	bdl	59	130	bdl	bdl	bdl	12	bdl	bdl
LD2	bdl	bdl	bdl	bdl	70	13	21	bdl	77	17	bdl	bdl	12	16	bdl	bdl	bdl
LD3	bdl	bdl	bdl	bdl	148	89	50	bdl	bdl	bdl	17	56	45	30	bdl	bdl	bdl
LD4	bdl	bdl	bdl	bdl	118	24	bdl	bdl	124	88	146	49	34	bdl	18	bdl	bdl
LD5	bdl	bdl	bdl	bdl	231	bdl	86	13	bdl	125	229	bdl	bdl	bdl	bdl	20	bdl
LD6	bdl	bdl	bdl	14	213	bdl	38	38	bdl	165	280	bdl	bdl	bdl	bdl	bdl	bdl
LD7	bdl	bdl	bdl	35	212	46	116	15	29	14	92	bdl	bdl	bdl	27	bdl	bdl
LD8	bdl	bdl	bdl	31	306	21	32	bdl	70	54	46	28	bdl	bdl	bdl	bdl	bdl
LD9	bdl	bdl	bdl	bdl	160	29	101	bdl	79	88	87	bdl	bdl	bdl	bdl	bdl	bdl
LD11	bdl	bdl	bdl	bdl	213	bdl	bdl	bdl	111	145	191	34	bdl	bdl	bdl	bdl	bdl
LD12	bdl	bdl	bdl	bdl	148	31	bdl	12	bdl	123	271	7	3	bdl	bdl	bdl	bdl
LD13	bdl	1	bdl	bdl	259	67	176	30	62	77	72	bdl	bdl	28	4	2	bdl
LD14	bdl	bdl	bdl	bdl	101	93	472	61	31	14	11	bdl	bdl	6	bdl	1	bdl
MC1	bdl	bdl	bdl	bdl	82	54	192	24	102	bdl	107	9	bdl	24	9	bdl	bdl
MC6	bdl	bdl	bdl	bdl	330	bdl	114	75	109	83	200	17	7	bdl	bdl	bdl	bdl
MC12	bdl	bdl	bdl	bdl	179	35	bdl	bdl	bdl	141	211	bdl	bdl	bdl	3	1	bdl

Sample	SnO_2	Sb_2O_3	TeO_2	Cs_2O	BaO	La_2O_3	CeO_2	Nd_2O_3	HfO_2	Ta_2O_5	WO_3	PtO_2	Au	HgO	PbO	Bi_2O_3	ThO_2
MC18	bdl	bdl	bdl	bdl	32	20	8	bdl	bdl	17	95	8	3	5	7	bdl	bdl
YW1	bdl	bdl	bdl	bdl	144	47	144	48	bdl	141	251	1	bdl	bdl	bdl	bdl	bdl
YW2	bdl	12	bdl	bdl	35	22	96	12	85	130	261	36	20	bdl	bdl	bdl	bdl
YW3	bdl	bdl	bdl	bdl	133	53	bdl	bdl	bdl	145	258	bdl	bdl	11	bdl	4	bdl
YW4	bdl	27	bdl	bdl	554	16	bdl	70	76	157	457	14	bdl	bdl	139	bdl	bdl
YW5	bdl	bdl	bdl	bdl	180	64	202	84	99	51	83	15	21	bdl	bdl	bdl	bdl
YW6	bdl	1	bdl	24	200	9	16	bdl	44	128	226	bdl	bdl	bdl	bdl	bdl	12
YW7	bdl	bdl	bdl	bdl	110	bdl	bdl	bdl	bdl	109	109	bdl	11	18	1	4	bdl

Supplementary materials II SEM-EDS and WD-XRF analysis of CRMs

BHVO-2, BCS-2 CRMs and NIST 1412 are polished blocks. The rest of CRMs are pressed powder pellets, which is reflected in higher errors and lower analytical totals due to mineralogical effects and porosity. Trace elements are below detection limits in all cases and thus the tables only report values higher than 0.1%.

Swedish Slag

	Na_2O	Al_2O_3	SiO_2	K_2O	CaO	TiO_2	MnO	FeO	*Total*
	wt%	wt%	wt%	wt%	wt%	wt%	wt%	wt%	wt%
Normalised reference values	0.64	7.76	25.82	1.03	1.52	0.32	3.27	59.63	95.76
MEASUREMENTS (NORMALISED)									
09/06/2013	0.9	7.6	24.6	1.3	1.7	0.3	3.1	60.5	88.8
03/06/2014	1.1	8.3	24.0	1.4	1.8	0.4	3.2	59.9	88.9
14/07/2014	1.0	7.5	23.4	1.3	1.6	0.3	3.5	61.3	86.0
08/12/2014	1.0	7.4	23.9	1.3	1.5	0.3	3.1	61.5	86.5
03/03/2015	1.2	7.6	24.4	1.2	1.6	0.4	3.5	60.1	91.1
22/06/2015	1.0	7.6	24.8	1.2	1.7	0.2	2.9	60.7	90.0
Mean	1.0	7.7	24.2	1.3	1.6	0.3	3.2	60.6	
PRECISION									
Standard deviation	0.1	0.3	0.5	0.1	0.1	0.1	0.2	0.6	
Coefficient of variation (%)	17	4	2	8	6	17	7	1	
ACCURACY									
Absolute error	0.4	-0.1	-1.6	0.2	0.1	0.0	1.0	0.4	
Relative error	62	-1	-6	24	8	-1	2	1	

Kresten, P., & Hjärthener-Holdar, E. (2001). Analysis of the Swedish ancient iron reference slag W-25:R. *Historical Metallurgy*, 35 (48-51).

BHVO-2 Basalt, Hawaiian Volcanic Observatory

	Na_2O	MgO	Al_2O_3	SiO_2	P_2O_5	K_2O	CaO	TiO_2	MnO	FeO	Total
	wt%	wt%	wt%	wt%	wt%	wt%	wt%	wt%	wt%	wt%	wt%
Normalised reference values	2.25	7.33	13.69	50.61	0.27	0.53	11.56	2.77	0.17	11.26	98.6
MEASUREMENTS (NORM.)											
09/06/2013	2.1	6.7	13.0	49.7	1.1	0.5	11.5	2.6	0.5	11.1	98.8
03/06/2014	2.3	6.8	12.5	49.0	1.0	0.5	11.6	2.9	0.4	11.3	98.4
14/07/2014	2.3	7.0	12.7	49.6	0.9	0.6	11.4	2.5	0.4	10.8	98.1
08/12/2014	2.2	6.9	12.6	49.2	1.1	0.6	11.3	2.4	0.3	11.2	97.9
03/03/2015	2.6	6.8	12.6	49.7	1.0	0.5	11.5	2.6	0.4	11.9	99.6
22/06/2015	2.3	7.3	12.7	49.6	1.2	0.5	11.1	2.7	0.6	11.5	99.4
Mean	2.3	6.9	12.7	49.5	1.0	0.5	11.4	2.6	0.4	11.3	98.7
PRECISION											
Standard deviation	0.1	0.2	0.2	0.3	0.1	0.0	0.2	0.2	0.1	0.3	
Coefficient of variation (%)	6	3	1	1	11	9	2	6	22	3	
ACCURACY											
Absolute error	0.1	-0.4	-1.0	-1.2	0.8	0.0	-0.2	-0.1		0.0	
Relative error	4	-6	-7	-2	285	-2	-1	-5		0.2	

United States Geological Survey (USGS), 1998. Certificate of Analysis: Basalt, Hawaiian Volcanic Observatory, BHVO-2.

http://crustal.usgs.gov/geochemical_reference_standards/basaltbhvo2.html#bibliography

BCR-2

	Na_2O	MgO	Al_2O_3	SiO_2	P_2O_5	K_2O	CaO	TiO_2	FeO	*Total*
	wt%	wt%	wt%	wt%	wt%	wt%	wt%	wt%	wt%	wt%
Norm. ref. values	3.22	3.65	13.74	55.05	0.36	1.82	7.24	2.30	12.63	98.28
MEASUREMENTS (NORM.)										
09/06/2013	3.3	3.5	13.0	55.6	0.4	1.8	7.4	2.3	12.6	99.1
03/06/2014	3.3	3.7	13.1	55.7	0.3	1.9	7.2	2.3	12.7	99.6
14/07/2014	3.3	3.3	13.0	55.4	0.4	1.9	7.4	2.5	12.7	98.5
08/12/2014	3.2	3.6	12.9	55.9	0.4	1.7	7.4	2.3	12.6	98.5
03/03/2015	3.3	3.7	13.1	55.2	0.6	1.8	7.4	2.2	12.8	99.5
22/06/2015	3.6	3.6	12.8	55.9	0.5	1.7	7.2	2.4	12.2	99.4
Mean	3.3	3.6	13.0	55.6	0.4	1.8	7.3	2.4	12.6	
PRECISION										
Standard deviation	0.1	0.1	0.1	0.3	0.1	0.1	0.1	0.1	0.2	
Coefficient of var. (%)	4	4	1	1	26	4	2	5	2	
ACCURACY										
Absolute error	0.1	-0.1	-0.8	0.6	0.1	0.0	0.1	0.1	0.0	
Relative error	3	-2	-5	1	15	-1	1	2	-0.2	

United States Geological Survey (USGS), 1998. Certificate of Analysis: Basalt, Columbia River, BCR-2.

http://crustal.usgs.gov/geochemical_reference_standards/pdfs/basaltbcr2.pdf

NCS Clay DC60105

	Na_2O	MgO	Al_2O_3	SiO_2	K_2O	CaO	TiO_2	FeO	*Total*
	wt%	wt%	wt%	wt%	wt%	wt%	wt%	wt%	wt%
Normalised reference values	1.92	1.95	14.08	70.67	2.82	3.43	0.70	4.43	94.30
MEASUREMENTS (NORMALISED)									
09/06/2013	1.9	2.5	16.6	64.9	3.2	3.9	0.9	6.3	82.7
03/06/2014	2.0	2.5	16.2	65.2	3.2	4.1	0.9	6.0	81.7
14/07/2014	1.7	2.7	16.3	64.4	3.3	4.3	0.8	6.4	82.8
08/12/2014	1.9	2.5	16.2	65.3	3.2	4.0	0.6	6.4	81.3
03/03/2015	2.0	2.5	17.0	65.3	3.2	3.8	0.7	5.5	83.0
22/06/2015	1.9	2.5	16.5	64.9	3.3	4.4	0.8	5.9	82.2
22/06/2015	1.8	2.6	16.7	64.2	3.3	4.2	0.8	6.4	83.5
Mean	1.9	2.5	16.5	64.9	3.2	4.1	0.8	6.1	
PRECISION									
Standard deviation	0.1	0.1	0.3	0.4	0.1	0.2	0.1	0.3	
Coefficient of variation (%)	6	4	2	1	2	5	13	6	
ACCURACY									
Absolute error	-0.1	0.6	2.4	-5.9	0.6	0.7	0.1	1.7	
Relative error	-4	29	17	-8	22	19	10	38	

https://www.labmix24.com/extern/downloadpdfdetails/32203/

NIST 76a Burnt Refractory

	MgO	*Al_2O_3*	*SiO_2*	*K_2O*	*TiO_2*	*FeO*	*Total*
	wt%	wt%	wt%	wt%	wt%	wt%	wt%
Normalised reference values	0.53	39.13	55.51	1.34	2.05	1.46	98.90
MEASUREMENTS (NORMALISED)							
09/06/2013	0.5	37.8	55.8	1.5	2.3	2.2	84.8
03/06/2014	0.3	37.6	56.0	1.5	2.5	2.1	85.7
14/07/2014	0.5	37.7	56.1	1.4	2.3	1.9	87.7
08/12/2014	0.4	38.0	56.5	1.3	2.0	1.8	86.8
03/03/2015	0.5	38.0	56.1	1.5	2.3	1.6	86.9
22/06/2015	0.6	38.4	55.7	1.4	2.1	1.9	85.7
Mean	0.5	37.9	56.0	1.4	2.3	1.9	
PRECISION							
Standard deviation	0.1	0.3	0.3	0.1	0.2	0.2	
Coefficient of variation (%)	19	1	1	6	9	10	
ACCURACY							
Absolute error	-0.1	-1.2	0.5	0.1	0.2	0.5	
Relative error	-12	-3	1	6	10	32	

National Institute of Standards & Technology (NIST), 1992. Certificate of Analysis – Standard Reference Materials 76a, 77a, and 78a Burnt Refractories. Gaithersberg, Maryland: ASTM/NIST.

https://www-s.nist.gov/srmors/view_det0.120ail.cfm?srm=76a

NIST 1412, multi-component glass

Light oxides Li_2O (4.53%) and B_2O_3 (4.50%) present in the certified composition cannot be detected by EDS.

	Na_2O	*MgO*	*Al_2O_3*	*SiO_2*	*K_2O*	*CaO*	*ZnO*	*SrO*	*CdO*	*BaO*	*PbO*	*Total*
	wt%	wt%	wt%	wt%	wt%	wt%	wt%	wt%	wt%	wt%	wt%	wt%
Norm. ref. values	5.18	5.18	8.31	46.85	4.58	5.01	4.95	5.03	4.84	5.16	4.86	
MEASUREMENTS (NORM.)												
09/06/2013	6.0	5.0	7.8	47.2	4.0	5.1	4.9	4.6	5.2	5.1	5.2	89.0
03/06/2014	5.9	4.5	8.0	47.5	4.4	4.9	4.7	4.9	4.9	5.2	4.9	90.5
14/07/2014	5.5	4.8	8.0	46.4	4.1	5.3	5.6	4.8	5.2	5.0	5.3	92.2
08/09/2014	6.1	4.6	8.0	47.1	4.5	5.0	5.1	4.3	5.0	5.2	5.2	91.4
10/10/2014	6.0	4.9	7.9	46.2	5.0	5.0	4.9	5.0	4.7	5.4	4.9	90.3
08/12/2014	5.9	4.8	8.0	47.4	4.3	4.9	5.1	4.7	4.6	5.2	4.9	91.4
03/03/2015	5.5	4.7	7.5	47.4	4.4	5.2	4.7	5.1	5.0	5.5	4.9	90.6
01/04/2015	5.4	4.9	8.1	46.8	4.9	5.0	4.9	4.5	5.0	5.5	5.1	91.7
22/06/2015	5.9	4.9	8.0	46.5	4.5	5.0	4.7	5.0	5.2	5.3	5.1	91.9
Mean	5.8	4.8	7.9	46.9	4.5	5.0	5.0	4.8	5.0	5.3	5.0	
PRECISION												
Standard dev.	0.3	0.1	0.2	0.5	0.3	0.1	0.3	0.3	0.2	0.2	0.1	
Coeff. of var.	5	3	2	1	7	2	6	6	4	3	3	
ACCURACY												
Absolute error	-0.6	0.4	0.4	-0.1	0.1	0.0	0.0	0.2	-0.1	-0.1	-0.2	
Relative error	-12	8	5	0	2	-1	0	5	-3	-2	-4	

https://www-s.nist.gov/srmors/certificates/1412.pdf

WD-XRF analysis of CRMs

Swedish slag

	Na_2O	MgO	Al_2O_3	SiO_2	P_2O_5	SO_3	K_2O	CaO	TiO_2	V_2O_5	Cr_2O_3	MnO	FeO	SrO	ZrO_2	BaO	La_2O_3	CeO_2	Total
	wt%	wt%	wt%	wt%	wt%	wt%	wt%	wt%	wt%	wt%	wt%	wt%	wt%	wt%	wt%	wt%	wt%	wt%	wt%
Normalised reference values	0.63	0.42	7.67	25.53	0.27	0.10	1.02	1.51	0.32	0.03	0.01	3.23	59.12	0.01	0.01	0.08	0.01	0.03	96.89
MEASUREMENTS (NORMALISED)																			
10/04/2014	0.86	0.28	7.95	22.73	0.25	0.14	1.02	1.29	0.25	0.03	0.02	3.19	61.78	0.01	0.02	0.11	0.02	0.05	90.20
18/11/2014	0.85	0.27	7.88	22.82	0.24	0.13	1.03	1.32	0.25	0.02	0.01	3.14	61.86	0.01	0.02	0.12	0.01	0.03	90.20
Mean	0.86	0.27	7.91	22.78	0.24	0.13	1.03	1.31	0.25	0.03	0.01	3.16	61.82	0.01	0.02	0.12	0.01	0.04	
PRECISION																			
Standard deviation	0.0	0.0	0.1	0.1	0.0	0.0	0.0	0.0	0.0	0.0	0.0	0.0	0.1	0.0	0.0	0.0	0.0	0.0	
Coefficient of variation (%)	2	0	1	0	4	5	1	1	0	24	30	1	0	4	0	2	18	39	
ACCURACY																			
Absolute error	0.23	-0.15	0.24	-2.75	-0.02	0.03	0.00	-0.20	-0.07	0.00	0.00	-0.07	2.70	0.00	0.00	0.04	0.00	0.01	
Relative error	36	-35	3	-11	-9	30	0	-13	-22	-11	29	-2	5	46	23	51	47	16	

BHVO-2 Basalt, Hawaiian Volcanic Observatory

	Na_2O	MgO	Al_2O_3	SiO_2	P_2O_5	K_2O	CaO	TiO_2	V_2O_5	Cr_2O_3	MnO	Fe_2O_3	Total
	wt%	wt%	wt%	wt%	wt%	wt%	wt%	wt%	wt%	wt%	wt%	wt%	wt%
Normalised reference values	2.21	7.21	13.46	49.73	0.27	0.52	11.36	2.72	0.06	0.04	0.17	12.26	100.33
MEASUREMENTS (NORM.)													
10/04/2014	2.48	5.40	16.45	48.77	0.26	0.51	10.69	2.24	0.08	0.06	0.18	12.88	86.80
ACCURACY													
Absolute error	0.26	-1.81	2.99	-0.97	-0.01	0.00	-0.67	-0.48	0.03	0.02	0.01	0.62	
Relative error	12	-25	22	-2	-2	-1	-6	-18	48	50	9	5	

NIST76a Burnt Refractory

	Na_2O	MgO	Al_2O_3	SiO_2	P_2O_5	K_2O	CaO	TiO_2	Fe_2O_3	SrO	Total
	wt%	wt%	wt%	wt%	wt%	wt%	wt%	wt%	wt%	wt%	wt%
Normalised ref. values	0.07	0.52	38.88	55.16	0.13	1.34	0.22	2.04	1.61	0.04	99.58
MEASUREMENTS (NORM.)											
10/04/2014	0.06	0.63	39.22	54.83	0.12	1.34	0.21	1.73	1.81	0.05	86.90
18/11/2014	0.06	0.65	39.17	54.91	0.12	1.34	0.21	1.73	1.78	0.05	87.00
Mean	0.06	0.64	39.20	54.87	0.12	1.34	0.21	1.73	1.79	0.05	
PRECISION											
Standard deviation	0.00	0.01	0.04	0.06	0.00	0.00	0.00	0.00	0.02	0.00	
Coefficient of variation (%)	2	1	0	0	2	0	1	0	1	2	
ACCURACY											
Absolute error	-0.01	0.12	0.31	-0.29	-0.01	0.01	-0.01	-0.31	0.18	0.01	
Relative error	-17	22	1	-1	-6	1	-5	-15	11	25	